The carbonate mass transport deposits of the Paleogene Friuli Basin (Italy/Slovenia): internal anatomy and inferred genetic processes

The carbonate mass transport deposits of the Paleogene Friuli Basin (Italy/Slovenia): internal anatomy and inferred genetic processes

Ogata, K.[1,a], Pogačnik, Ž.[2], Pini, G.A.[3], Tunis, G.[3], Festa, A[4], Camerlenghi, A[5] and Rebesco, M.[6]

[1] Department of Arctic Geology, University Centre in Svalbard, P.O. Box 156, 9171, Longyearbyen, Norway (kei.ogata@gmail.com)

[2] Salonit Anhovo, Building materials, Joint-Stock Co., Anhovo 1, 5210-Deskle, Slovenia (zeljko.pogacnik@salonit.si)

[3] Dipartimento di Matematica e Geoscienze, Università di Trieste, 34128 - Trieste, Italy (gpini@units.it; tunis@units.it)

[4] Dipartimento di Scienze della Terra, Università di Torino, 10125 Torino, Italy (andrea.festa@unito.it)

[5] Department of Geophysics and Marine Geology, Istituto Nazionale di Oceanografia e Geofisica Sperimentale (OGS), 34010 - Trieste, Italy (acamerlenghi@ogs.trieste.it)

[6] Development of technology and marine research (RIMA), Istituto Nazionale di Oceanografia e Geofisica Sperimentale (OGS), 34010 - Trieste, Italy (mrebesco@ogs.trieste.it)

[a] present address: Dipartimento di Fisica e Scienze della Terra "Macedonio Melloni", Università degli Studi di Parma, Campus Universitario - Parco Area delle Scienze 157/A, I-43124 Parma, Italy (kei.ogata@unipr.it)

Abstract

The Paleogene carbonate "megabreccia" units of the Friuli Basin are composite deposits produced by catastrophic shallow-water carbonate platform collapses re-deposited in relatively deep-water inner foredeep settings developed at the front of the advancing Dinaric thrust system. These thick, basin-wide mass transport deposits (MTDs) record the catastrophic emplacement of bipartite slide masses, comprising a lower coherent/cohesive blocky flow and an upper grain/turbulent flow. We here present the results of micro- to outcrop-scale structural analyses, constrained by stratigraphic and sedimentologic observations, performed to identify the internal deformation mechanisms and the emplacement processes of four of the largest MTDs exposed in two large three-dimensional outcrops: the Vernasso (NE Italy) and Anhovo (W Slovenia) open-pit quarries. Our results reveal a variety of primary (sedimentary) soft sediment deformation structures testifying fluid overpressure conditions within the brecciated, fine grained matrix that sustain, intrude and surround slide blocks and clasts. Meso-scale structural analyses unraveled paleo-transport directions toward the N for the Vernasso quarry and toward the S for the Anhovo quarry. This suggests a forced propagation of the mass transport events controlled by the shape of basin, and reinforces the interpretation of different source areas related to multiple collapses from a carbonate platform rimming the southeastern tip of the basin. These units are thought to represent exhumed fossil examples of the MTDs extensively mapped in the present-day, carbonate-dominated continental margins, and thus, considered as reliable analogues for integrated studies.

Keywords: carbonate mass transport deposits; syn-sedimentary deformation; slide blocks; sedimentary matrix; sedimentary injections

1. Introduction

Basin-wide deposits that originated from submarine landslides and slope failures largely crop out in the sedimentary record of mountain chains worldwide (see, among many others, Arnaud and Eyles, 2002; Lucente and Pini, 2003, 2008; Alonso *et al*., 2006; Burg *et al*., 2008; Callot *et al*., 2008a; Van der Merwe *et al*., 2009; Alves and Lourenco, 2010; Yamamoto *et al*., 2009; Codegone *et al*., 2012; Ogata *et al*., 2012a). These deposits represent either the products of a single depositional event (mass transport deposit, MTD) or composite bodies originated by subsequent superposed events (Lucente and Pini, 2003; Ogata *et al*., 2012a; 2012b). The latter are defined as mass transport complexes (MTCs), following the seismo-stratigraphic definitions introduced by Weimer (1989). Each individual deposit is often partitioned in different parts characterized by specific deformational styles and interpreted as products of discrete masses moving differentially, and, more generally as the result of the coexistence of more submarine *en-masse* flow processes (Strachan, 2002; Lucente and Pini, 2003; Ogata *et al*., 2012a). From the point of view of the internal structures and kinematics, the lower slide surface and the shear zones separating the individual masses inside the body are characterized by different structural associations, ultimately suggesting different mechanism of movement (Pini *et al*., 2012). Among the possible mechanisms, the dispersive force due to the grain-to-grain interactions (Middleton and Hampton, 1973; Melosh, 1987) and the interstitial fluid overpressure within a hyperconcentrated sedimentary matrix (Mutti, 1992; Mutti *et al*., 2006; Callot *et al*., 2008b; Ogata *et al*., 2012a; 2012b) are the most likely.

The Paleogene carbonate "megabreccias" of the eastern Friuli (Italy) and western Slovenia are thick and laterally extensive mass transport deposits (MTDs hereafter), originated from the accumulations of heterogeneously-sized carbonate debris, with the largest bodies being up to 260 m thick and up to 100 km wide. They represents repeated catastrophic submarine landslide events (Tunis and Venturini, 1992; Catani and Tunis, 2001), in which large sectors of shallow-water carbonate platform collapsed and re-deposited in a complex, deep-water, elongated turbidite-filled foredeep basin system (Friuli Basin of Buser, 1987 and Placer *et al*., 2010; Julian Basin, or Friuli Paleogene Basin of Selli, 1953 and Gnaccolini, 1968).

The type and the scale of the sedimentary processes inferred for the largest MTD units, as well as the size of the component slide blocks (i.e. olistoliths) are comparable with the seismic analogues documented by the current marine geology surveys in which, however, the limited geophysical resolution fails in detailing meso-scale internal and basal features. Nonetheless such impressive characteristics, these bodies are still relatively poorly understood in terms of sedimentary processes and overall significance.

We here present the results of analyses performed on the Vernasso (Italy) and Anhovo (Slovenia) quarries where four of the largest MTDs are outstandingly exposed: the Vernasso unit and the overlying Porzus unit on the Italian side (early Eocene; Catani and Tunis, 2001), and the Rodež and the overlying Perunk units on the Slovenian side (late Paleocene; Pogačnik et al, 2009). The aim of this work is to provide a general model for the transport-emplacement of this kind of MTDs (type 2 of Pini *et al*., 2012), which are characterized by 1) the largest amount of involved sediments in a single event, 2) the highest paleo-transport velocity, and 3) the strongest deformation of the substratum. The paleogeographic significance of the bodies in the Paleocene-Eocene Dinaric wedge-foredeep system is only preliminary discussed, since it is not the main goal of this work. Importantly, the studied cases of exhumed MTDs, represent analogues of present-day MTDs extensively mapped along carbonate-dominated continental margins. Hence, our findings may provide important constraints to the internal structure and processes of formation of such sedimentary bodies, otherwise hardly solvable through the standard geophysical tecniques.

2. Geological setting

The investigated MTDs are located in the southwest-verging Northern External Dinarides thrust belt (Placer, 1981; Merlini *et al*., 2002), embedded in the stratigraphic succession of the Friuli Basin, which structurally pertains to the highest thrust sheet of the External Dinaric Thrust Belt (fig. 1), the Trnovo nappe (Placer, 1981; Placer *et al*, 2010). The present day Mesozoic to Paleogene rock

exposures in the study area define a NW-SE striking regional-scale monocline dipping toward the SW likely due to later tectonic tilting contemporary and connected to the NW-SE trending ("Dinaric") thrusts, faults and folds (figs. 1, 2). The latter formed localized domains of intense deformation (see Tunis and Pirini Radrizzani, 1987) and belts of vertical or high angle overturned bedding (Carulli, 2006; Zanferrari et al., 2008, 2013). However, areas of almost undisturbed beds largely prevail (see e.g. Skaberne, 1987) and let the MTDs and other key beds to be traced and mapped at the scale of the entire basin, as it is preserved nowadays. Figures 2 and 3 show the tentative correlation of three of the largest MTDs, the Vernasso, Mt. Ioanaz and Rodež units, based on the existing literature and maps (Feruglio, 1925; Pirini *et al*., 1986; Tunis and Pirini Radrizzani, 1987; Skaberne, 1987; Tunis and Venturini, 1992; Sartorio *et al*., 1997; Catani and Tunis, 2001; Perricone, 2003; Carulli, 2006) and unpublished stratigraphic data. In the proposed framework, Mt. Ioanaz and Rodež units may be considered as coeval (Pirini *et al*., 1986; Pogačnik *et al*., 2009), even if a direct correlation needs to be confirmed (see figs. 2, 3).

From a paleogeographic point of view, since Late Cretaceous (late Campanian) to Middle Eocene, the former extensional Julian-Slovenian Basin (Šmuc, 2005; Rožič and Šmuc, 2011) and the surrounding Julian High and Friuli (Dinaric) Carbonate Platform evolved in an articulated foredeep system due to the lithospheric flexural stages caused by the SW-directed advancement of the migrating front of the Dinaric Thrust Belt (connecting the Dinarides with the Western Carpathians-Alps systems; Csontos and Vörös, 2004). The geometry of the depositional setting evolved, therefore, in an elongated basin (Friuli Basin, Buser, 1987) now oriented NW-SE (Placer, 1981; 1998; Placer *et al*, 2010), confined by a shallow-water and partly emergent carbonate platform to the SW and S, the Dinaric deformational wedge to the NE and the embryonic Alpine system to N (Pirini *et al*., 1986; Tunis and Pirini Radrizzani, 1987; Tunis and Venturini, 1992; Catani and Tunis, 2001; see fig. 3C). The migration of the external (in orogenic sense) Dinarides has been also responsible for the progressive SW-ward shift of the entire basin-slope system and of the depocenter of the flysch deposits (Piccoli and Proto Decima, 1969; De Capoa and Radoicic, 2002),

which become progressively younger to the SW. However, in the Iudrio valley (Sartorio *et al*., 1997) and the Anhovo and Soča-Idrijca area, the Late Cretaceous to the earliest Eocene flysch beds (including the Ypresian Mt. Ioanaz and the Rodež and Perunk MTDs, figs. 2, 3) wedge-out and close laterally toward S and E, showing onlapping relationships with the underlying carbonate platform through a marked unconformity (Kuščer *et al* 1974, Skaberne, 1987). Either this area may represent the true edge of the Late Cretaceous-earliest Eocene basin, or a system of NNE-SSW oriented intrabasinal highs depicting a physiographic threshold between a NW and a SE sub-basin, as suggested for the Eocene (late Cuisian) by Pirini *et al*. (1986). A strong control on the MTDs paleo-transport and sedimentation by NE-SW oriented transfer faults has been also suggested by Venturini and Tunis (1992).

In terms of sediment dispersal pathways, the vast majority of the turbiditic flows spread out along the axis of the flysch basins, mostly in relation of its confined, elongated shape, as suggested by strong coherencies of the paleo-current data from NW (Venzo and Brambati, 1969; Kuščer *et al*., 1974; Pirini *et al*., 1986; Tunis and Pirini Radrizzani, 1987; Catani and Tunis, 2001; Perricone, 2003). This paleo-current trend is typical of the siliciclastic turbidites, but also the calciturbidites and the calcareous microbreccias, sourced from the southwestern and northeastern basinal margins, show this trend, being the flow redirected along the axis of the highly confined basin (Tunis and Venturini, 1992). However, some hybrid turbidites show paleo-currents directions from NE (Venturini and Tunis, 1992; Catani and Tunis, 2001) and some thick calcareous turbidites from SW, both flowing in directions almost orthogonal to the basin axis (Catani and Tunis, 2001; see fig. 3C).

The MTDs are also fining and thinning toward N (Tunis and Venturini, 1992), with the exception of the eastern Anhovo area where beds thin toward the W (Kuščer *et al*., 1976; Skaberne, 1987). Data from recumbent slump folds in the MTD basal intervals display axial directions with a dispersion from NW-SE to NNE-SSW (Pirini *et al*., 1986; Ponton e Turco, 1997; Perricone, 2003); these data, interpreted with the mean axis method, let these authors to suggest a transport toward NE and E, in reason to the eastern-verging folds. However, some data collected from the north-easternmost side

of exposition of the Mt. Ioanaz MTD (between Natisone and Iudrio valleys) suggest a NW-directed transport (Perricone, 2003). Multiple source system is also suggested from the arenites' and rudites' composition, with three main groups, as defined in the literature (Kuščer *et al*., 1974; Pirini *et al*., 1986; Skaberne, 1987; Tunis and Pirini Radrizzani, 1987, Tunis and Venturini, 1992, Venturini and Tunis, 1992; Catani and Tunis, 2001) and described hereafter in order of relative abundance (see fig. 3C): 1) dominantly siliciclastic "Alpine and Carnian input" from NW-N, 2) extra- and intra-bacinal carbonatic "Friuli input" from SW and S, 3) mixed "Wedge-chain input" from NE.

A combination of all these elements depicts a complex paleo-physiographic setting during the Paleogene, with multiple sediment inputs radially converging into an elongated narrow basin characterized by an articulated system of internal depocenters. Even if some preliminary considerations may be pointed out on the basis of our findings, a comprehensive compilation of the complex structural-stratigraphic relationships of this sector of the northwestern Dinaric system is well beyond the scope of this contribution.

3. Basic observations and methods

The Paleocene-Eocene sedimentary succession recorded within these basins is identified with the informal name of Grivò Flysch unit in Italy and the corresponding Kožbana Flysch unit on the Slovenian side (Tunis and Venturini, 1997), and it contains at least 25 major carbonate MTDs (Feruglio, 1925). These bodies are intercalated in the middle-lower part of the succession (i.e. middle-late Paleocene) within a background sedimentation comprising carbonate, siliciclastic and mixed turbidites deposited in a mid-water depth, base of slope-basin plain setting (Tunis and Venturini, 1997). Such carbonate megabeds fall in the field of the so-called "megabreccias", "megaturbidites" or "olistolith swarms", following and summarizing the definitions and interpretations developed by Johns *et al*. (1981), Seguret *et al*. (1984), Labaume (1992) and Spence and Tucker (1997).

The thickness of the investigated MTDs (see fig. 3A) spans from tens of meters to the maximum values of 264 meters for the Vernasso unit (identified as "megabed" or MB 11 by Catani and Tunis, 2001) and about 300-400 meters for the Rodež unit (Skaberne, 1987). Their internal organization is characterized by recurrent subdivisions with generally transitional contacts (fig. 3B), defined from base to top as (Tunis and Venturini, 1992; Marjanac, 1996; Catani and Tunis, 2001): i) calcareous breccia with oversized carbonate olistoliths (U1), ii) calcareous breccia with bedded siliciclastic-carbonate and marly olistoliths (U2), iii) graded calcareous breccia, calcirudite (U3), iv) graded, laminated calcarenite (U4), and v) massive/laminated marlstone.

As for the provenance and the age of the detritus in the MTDs, the limestone debris indicates a sedimentary source from old and penecontemporaneous shallow-water carbonate platforms, which were located mostly along the southern margin of the late Paleocene-early Eocene flysch trough (Pirini *et al*., 1986; Tunis and Venturini, 1992) or to the E (Skaberne, 1987). The lithology of the olistoliths and blocks in the MTDs embrace sequences dated back to early Cretaceous up to early Eocene (e.g. Vernasso MTD). The source is likely from the Friuli Carbonate Platform (Cati *et al*., 1987), which was largely buried under the thick post-early Eocene clastic succession. Neverthless, the clast nature both in Anhovo and Vernasso debrites can be easily recognized within the Cretaceous, Paleocene and early Eocene (e.g. Vernasso MTD) carbonate sections of the Karst region and surrounding areas, all pertaining to the Friuli Carbonate Platform (Pirini *et al*., 1986; Tunis and Venturini, 1992).

On the other hand, the finer-grained part of the matrix likely derives from the reworking and incorporation of the mixed siliciclastic-carbonate slope (ages spanning from the Hauterivian to the early Eocene; Catani and Tunis, 2001). The smaller bedded and plastically deformed blocks of the U2 are mainly sourced from intra-basinal units, almost coeval with the bodies' emplacement, representing ripped-up fragments from the substratum (Tunis and Venturini, 1992). This kind of partition is likely due to the frontal erosion of the substrate operated by the U1 and the consequent incorporation of the material in the U2, as suggested by Johns *et al* (1981), Seguret *et al*. (1984),

Labaume (1992) for the Eocene Jaca Basin carbonate megabeds of the south-central Pyrenees in Spain. This subdivision is summarized in fig. 3B.

In order to better describe the internal geometries of these bodies we collected mesoscopic structural data on 1) symmetric and asymmetric folds, 2) ductile, brittle/ductile and brittle structures, and 3) geometric/spatial distribution of the internal components (i.e. clasts, blocks and olistoliths), following the criteria proposed by Ogata *et al*. (2012b). The collected structural parameters are exemplified in fig. 4.

Fold axis orientation data (trend/plunge), have been plotted using the separation-arc method, and consequently represented as S- or Z-type (i.e. sinistral or dextral, respectively) on the basis of their down-plunge vergence (Hansen, 1971; Bradley and Hanson, 1998). Given the complex arrangement and shape of the investigated folds (i.e. rootless, recumbent and isoclinal sheath folds), the separation-arc method has been considered the most reliable even if not the most precise, rather than other methods (i.e., the mean axis, axial-planar intersection, fold-hinge azimuth and interlimb angle methods), which are instead better designed of typical slump folds, as outlined by Lucente and Pini (2003), Strachan and Alsop (2006), Debacker *et al*. (2009a; 2009b) and Ogata (2010). Wherever possible, we also collected the azimuth of long axes of sheath folds and the axes of double verging box-folds (trend/plunge) as complementary data to support the interpretations (see conceptual block diagram in fig. 4).

Ductile shear zones (D-type; *sensu* Passchier and Trouw, 2005) display plastic structures that are very similar to the "typical", tectonic, ductile shear zones/faults (mesoscopic ductile behavior; Pini, 1999) and, thus, the same terminology has been applied. Instead of a single, discrete slip plane these shear zones share the occurrence of centimeters to meters thick, discontinuous intervals where the bulk of the deformation is represented (see fig. 4). Brittle/ductile deformation is instead identified within slide blocks by sharp discontinuities such as wedge-shaped sediment injections and sedimentary veins developed at the lithologic boundaries, testifying marked competence contrast between the main slide elements. Given the roughly tabular- to oblate- and lozenge-shaped

appearance of the slide blocks, the geometric analysis of the internal components was performed collecting data on the internal bedding, main axial planes and imbrication relationships, along with other internal structures. Structural discontinuities, found both within the slide mass and the substrate, have been treated as planes and consequently collected in terms of strike/dip (see fig. 4). All of those above-mentioned structural elements are confined within the MTD body and its volume of influence within the host formation, and do not display any evidence of tectonic lineation (e.g. flexural slip-related slickenlines) and or foliation (e.g. folding-related cleavage). The data collected from single stations within the same body have been then combined to achieve a broader representative estimation of the paleo-transport direction for each MTD in the investigated section.

In both the study area, the host rock, even if fractured and veined, does not show any sign of syn-kinematic metamorphism, but is instead fractured and veined, developing typical brittle structures. The clear crosscut and angular/geometric relationships between the ductile-brittle/ductile features and the brittle ones constrain their structural (i.e. sedimentary vs. tectonic) evolution. Evidence of these later, "true" (i.e. tectonic) brittle deformation is provided by the occurrence of 1) systematic sets of joints, 2) calcite vein systems and 3) shear fracture networks (with kinematic indicators such as calcite steps, fibrous growth crystals, tension gashes and striations/slickenlines), and 4) stylolites, all of them affecting both the MTD body (i.e. internal slide elements and the matrix) and the host succession. Brittle shear zones (B-type) and thrusts have been observed to reactivate/rework preceding structural discontinuities such as original lithologic boundaries and ductile shear zones (D-type; see above), and thus collected to outline their spatial relationships.

Moreover, optical microscopy observations have been carried on thin sections coming from sedimentary matrix samples collected around the slide blocks and within the injections found in the Unit II in order to describe the main micro-structural and textural characteristics, used to identify the primary (i.e. sedimentary) deformation mechanisms. The integration of these results, coming from these different structural datasets, allow constraining the genetic processes and emplacement consequences.

4. Results

In the following sub-sections we present an outline of the investigated locations and the relative results case by case.

4.1 The Vernasso quarry (Italy)

The Vernasso quarry is located on the right-hand side of the Natisone Valley (46°7'5.30"N, 13°28'6.64"E), about 4 km to the NE of Cividale del Friuli, and represents the type locality of the MB 11 (Gnaccolini, 1968), offering clean and well preserved exposures on an area of about 0.33 km^2 (see fig. 2, 3). Here about the 90% of the of the Vernasso unit (MB 11) is exposed along with the overlying sedimentary succession (fig. 5A-C), made up by thin-bedded, siliciclastic and mixed turbidites with some very thick calcareous turbidites, including the other investigated MTDs (MB 15; fig. 5B-F).

The whole succession belongs to a monocline dipping about 20° toward SW, and it is bordered by NW-SE striking thrusts and normal faults (see figs. 2, 5), showing the same Dinaric-type direction (Tunis and Venturini, 1997). Apart such structures, the tectonic disturbance is minimal and no signs of pervasive tectonic deformation have been recognized in the investigated area and nearby, being preferentially localized at the boundaries of the principal thrust sheets/nappes.

Seven measurement areas representative of the upper part of the MB 11's unit U2 and the lower part of the MB 15's unit U1 (1 to 6, and 7, respectively; fig. 5C) have been investigated, where the meso-scale structures and the block-matrix relationships are better preserved. The upper units U3, U4 and U5, comprising the grain flow/turbulent-related part of the deposit (e.g. Tunis and Venturini, 1992), are not detailed in this study.

Slide blocks size spans from more than 100 m across in the U1 to 1-10 m in the U2. Their dimensions and shapes depend on the composition (carbonate *vs.* siliciclastic), texture (fine- *vs.* coarse-grained), fabric (massive/homogeneous *vs.* laminated/heterogeneous) and bedding type

(bedded *vs.* non-bedded, lenticular vs. tabular) of the involved deposits. Whatever the lithology, m-sized blocks are usually massive and correspond to single, detached thick bed, while blocks of 10-100 m across are made up of still stratified bedsets. Along with the larger dimensions, carbonate blocks also share sub-angular shapes (from the clast- to the slide block-scale) compared with the smaller and sub-rounded shapes of the siliciclastic ones (see fig. 5D-E).

The most representative mesoscopic structures (tens of cm- to tens of m-sized), are: 1) asymmetric folds, 2) breccia matrix injections (fig. 6A-E) and 3) low-angle ductile shear zones (fig. 6F-I). Moreover m-sized, interconnected normal fault-thrust systems can be observed in the substrate below the base of the MB 15 (fig. 7A-F). At the hand specimen scale, evidence of intrafolial folding, fluidal structures and localized sand-mud mixing have been observed within and around the slide blocks (i.e. olistoliths) floating in the breccia matrix.

Observed meso-scale folds are rootless, isoclinal, disharmonic, strongly non-cylindrical, recumbent synclines and anticlines developed at meters to tens of meter scale, commonly sharing thickened hinge zones. These folds, affecting both the matrix and the slide blocks, are usually developed in the hangingwall of low-angle ductile thrusts and shear zones (see fig. 6I). No associated syn-kinematic brittle features such as mineralized veins and slickenlines, or folding-related cleavage have been observed. Breccia injections (i.e. sedimentary dykes) are common around and inside slide blocks, and tens of m-sized, dome-shaped structures deforming the upper boundary of the U2 with the U3 have been observed (see fig. 6A-E). Systems of low-angle, ductile thrusts and shear zones are observed both within the matrix and the slide blocks (see e.g. fig. 6F-I). These features are usually marked by variable amount of matrix arranged in elongated lenses and bands along the plane of the shear zone, sometimes bearing pseudo-Sigma and other ductile kinematic indicators (see fig. 4).

Microscopic observations on thin sections from two oriented samples of the sedimentary matrix (both host and injected; fig. 8A-B and C-D, respectively) indicate a poorly sorted, mud-supported micro-breccia made up by angular to sub-rounded particles of different carbonate lithologies (e.g.

limestones, wackestones, packstones, grainstones, bioclastites, scattered bioclasts) contained within a mixed siliciclastic-carbonate pelitic material. It is characterized by an overall "particle-in-matrix" fabric, with localized variations in the amount of the finer grained component. No breakage at grain-to-grain contacts or syn-kinematic recrystallization has been observed, and most of the mineralized veins do not propagate into the surrounding matrix, resulting confined within the grains. On the other hand microinjections of matrix into fractures of rigid particles, plastically deformed pseudo-matrix intra-clasts and fluidal structures around competent clasts, suggest independent grain flow at low confining stress and overpressured fluid conditions as main deformation mechanism (fig. 8A-D).

Detailed analyses on the basal erosional contact and the related deformations of the underlying sediments (i.e. substratum) have been carried on below the MTD 15, due to the favorable outcrop condition (see fig. 7A-G). The substratum just below the olistolith is deformed by a system of spoon-shaped mesoscopic ductile faults composed by a listric normal part connecting with a frontal low-angle thrust, which accommodate few centimeters of displacement (see fig. 7C-E). Mechanical striations without associated mineralization/fracturing have been recognized and measured at the base of a marly olistolith in MB 15 (fig. 7G). Drag direction is revealed by the stratigraphic offset and by the systematic verging direction of cm- to tens of cm-sized, hinge-thickened folds (see fig. 7F), which are remarkably devoid of any folding-related cleavage, syn-kinematic calcite mineralization or slickenlines.

The above-mentioned structures are locally overprinted, crosscut and reworked (with an different shearing sense from the original) by brittle ones (see fig. 6F-I). The latter, represented by non-systematic joints and shear fractures marked by calcite mineralization (mainly as shear fibrous/stepped veins), stylolites and slickenlines, are coherent with the regional stress regime given by the Dinaric (ca. SW-NE) compression. It is important to stress that these brittle structures systematically affect the whole investigated sedimentary succession, while ductile ones are confined within and immediately around (particularly below) the MTD bodies. These strictly

tectonic features have been also measured and compared to the others to highlight their systematically different attitude with respect to the sedimentary ones (see below).

4.2 The Anhovo quarry (Slovenia)

The Anhovo quarry is located on the left-hand side of the Soča/Isonzo Valley (46°3'42.93"N, 13°37'58.14"E), about 20 km to the N of Nova Gorica, and it covers an area of about 1.3 km^2 (including the Rodež and Perunk quarry segments; fig. 9A-F). The area is bordered to the E by the Trnovo plateau and to the W by the Kanalski-Kolovrat ridge and it is crossed by two NW-SE regional faults (Buser, 1987; Pogačnik, 2010) separating the lower and upper Paleocene deposits, and affecting lower Cretaceous limestone (Skaberne, 1987). Apart the local tectonic disturbance related to these structures, the sedimentary succession is relatively undisturbed, dipping 20-40° toward the SW in an approximately homogeneous monocline through the entire area (see fig. 2). According to the tectonic framework, the area belongs to the Trnovo nappe, the same tectono-stratigraphic unit containing the Vernasso section (see fig. 1, 2, 3).

In this sector, a total of five measurement areas have been investigated, three for the Rodež quarry segment (see fig. 9C) and two for the Perunk quarry segment (see fig. 9B), covering at least four megabeds and associated interbedded sedimentary intervals. Following the local stratigraphic subdivision into single, recurrent litho-stratigraphic associations ("cyclothemes" made up by the single megabreccia units and the associated "normal" sedimentary cover proposed by Skaberne (1987), the investigated succession covers about four piled litho-stratigraphic associations (see fig. 9F). Since the economic interest of the cement and stone industry in the productive, high-quality marlstone (U5), calcirudite (U4) and calcarenite (U3) divisions (Pogačnik *et al*, 2009), these largest bodies have been extensively excavated (Pogačnik and Stupar, 2006) in relatively large open-pit quarries and thus outstandingly exposed in clean, laterally and vertically extensive, almost three-dimensional outcrops (see fig. 9A-C).

Structural analyses have been performed on the siliciclastic olistoliths and matrix of the U2

comprising the thickest Rodež unit and the overlying Perunk 1 unit (fig. 10), and the carbonate olistolith and the breccia matrix of the U1 of the uppermost Perunk 2 unit (fig. 11). In places, also structural data from the substrate (i.e. interbedded background sedimentation intervals) have been collected to unravel the syn-sedimentary deformations and their relationships with the MTDs and the paleo-slope (fig. 12).

Cretaceous limestone blocks and substrate rip-up olistoliths of more than 100 m in length and 30 m in height were found within the U1 of the Rodež unit. The carbonate olistoliths in the Perunk 2 unit, made up of exotic (i.e. extrabacinal) Cretaceous limestones and marlstones, and intrabasinal Paleocene-lower Eocene shallow water wackestones/packstones (Pogačnik, 2010), show sub-angular, lozenge-like shapes being always associated with relatively high amounts of breccia (see fig. 11E, H, I and J). On the other hand, the rip-up olistoliths comprising fragments of the coeval slope-basin plain sedimentary succession (including re-sedimented carbonates in form of smaller megabeds/megaturbidites) show more complex shapes, usually with low H/L ratio, being plastically deformed into detached, rootless folds (see fig. 9D and 10).

The slump-type folds (i.e. hinge-thickened, plastic folds without associated cathaclastic shearing, mineralization or cleavage) developed by these rip-up olistoliths share marked curvilinear axes, locally resulting in complex sheath folds (see for example fig. 10A and D). Liquefaction of sandy layers within the folded olistoliths is often observed, with the development of over-thickened fold hinges, and shear-related, layer-parallel asymmetric boudinage on the limbs (see fig. 10D). In turn, plastic shearing of the muddy intervals (e.g. pseudo-SC and Sigma-type structures) is commonly observed (fig. 10B, E and F). Notably, at the entire outcrop scale, an apparent internal partition of the structural elements within the U2 of the Rodež unit can be recognized, with synclinal folds dominating in the lower part and anticlinal folds in the upper part.

The associated sedimentary matrix comprises a generally mud-sustained carbonate breccia made up by angular and sub-angular carbonate elements (same lithologies of the slide blocks; see above) with variable amount of fine-grained, mixed siliciclastic-carbonate material. The amount of this

clayey-marly material is highest in the sedimentary matrix that characterizes the lower part of the deposit (see fig. 11H-J).

Within the U2, brittle/ductile structures such as sedimentary veins and injections of the background sedimentary breccia matrix into the olistoliths are commonly observed: wedge-shaped sedimentary intrusions are distributed radially to the folds' flexure axes (see fig. 9E), while pipe-shaped injectites are found at the base of larger slide blocks (fig. 11F and G) suggesting a relatively strong rheologic contrast between injected olistoliths and enclosing matrix.

The same structures are also found injected along the folds' axial planes, showing evidence of shearing coherent with the folding mechanism (e.g. asymmetric boudinage and pinch-and-swell arrangement, sigma-type and SC-type structures) and sometimes developing off-shooting secondary injections splaying out from the main one, especially close to the hinge zones (see fig. 10A). Moreover, cm- to m-sized cusps are observed to wedge downward injecting calcarentitic and calciruditic material from the U3 into the U2. At a larger scale, dome-like structures up to ten of meters in size are observed to deform the contact between the U2 and U3, creating marked thickness variations on short distances (fig. 10G).

Complex folds' interference patterns (i.e. refolding of earlier, previously-formed folds) and deformation of ductile and brittle/ductile discontinuities (e.g. folds' axial planes, shear zones, units' boundaries, matrix injections etc.) are documented. These deformations are well recorded in sedimentary injections showing the occurrence of ptygmatic folding, iso-directional bending, displaced segments and other generalized, pure and simple shear-related structures (see fig. 10C).

Microscopic observations confirm the absence of grain breakage at particle-to-particle contacts (i.e. cathaclasis) and syn-kinematic mineralization/veining. The most representative micro-scale features (at least for the analyzed bodies) are: 1) small scale injections of fine-grained material into particles, 2) fluidal, pseudo-deformation/disaggregation bands and 3) grain rotations ("galaxy structure"-type fabric of Phillips, 2006).

The sedimentary interval just above the Rodež unit has been also analyzed given the occurrence of

structures such as low angle thrusts, pseudo-SC structures and mesoscopic duplexes, which defect of any kind of brittle deformation suggesting an overall SW-directed layer-parallel shearing (see fig. 12B-H). These sedimentary intervals are characterized by the presence of m-thick, lens-shaped, deeply scouring carbonate breccia deposits and mixed-siliciclastic debris flow bodies, locally forming "channelized" architectures (see fig. 12A and I).

In the Perunk quarry segment, a well-exposed example of channelized breccia body is located about 10-15 m above the Perunk 2 unit: the sedimentologic characteristics are the same of the thick carbonate turbidite beds found elsewhere, but in this case the deposit shows an erosional base that deeply scours into the underlying succession of about 4-5 m (see fig. 9B and 11B). Due to the overall SW-directed dip, only one steep (about 40°) side of the erosional feature is cropping out and it is observed to flatten out rapidly becoming concordant with the bedding over short distance. Interestingly, the levee and the inferred axis of the channel are roughly parallel to the margin of the large carbonate olistolith that characterize the underlying Perunk 2 unit (see fig. 11B).

5. Discussion

In the next sub-sections we discuss the inferred deformation mechanisms and depositional processes responsible for the formation of the investigated MTDs, along with interpretations on the main paleo-transport directions. Considerations on the possible trigger mechanisms/pre-conditioning factors are also presented.

5.1 Deformation mechanisms

Whereas systematic brittle structures are observed to affect the whole investigated sedimentary succession, ductile and brittle/ductile structures are instead confined in the close proximity and within the MTDs. Mutual crosscutting relationships confirm that brittle structures overprint and thus postdate the ductile and brittle/ductile ones, sometimes reworking and reactivating with roughly opposite (Vernasso area) and concordant (Anhovo area) sense of shear the low-angle,

ductile discontinuities (see for example fig. 6A, G, H and I).

Ductile structures, observed both within the slide blocks and the matrix, are likely related to soft-sediment deformation acting within intervals characterized by weak competence contrast and passive plastic deformation of the elements. This is particularly evident in the matrix-dominated parts where detached slump-type folds with thickened hinge zones and plastically deformed intra-clasts are enclosed within a muddy micro-breccia characterized by hydro-plastic intrafolial folding and fluidal structures.

Brittle/ductile structures, largely represented by sedimentary veins and matrix injections, are mostly observed at the slide blocks' boundaries, testifying strong competence contrast between relatively rigid elements (i.e. slide blocks) and a liquefied medium (i.e. matrix). This kind of deformation is inferred to develop through the "pseudo-fracturing" of the relatively more competent material belonging to the slide blocks with consequent void creation and passive accommodation of the still liquefied sedimentary matrix into the newly formed space. This difference in the competence contrast is thought to testify the progressive rheologic evolution of the internal slide elements from the syn-depositional phase, represented by the ductile products, to the early post-depositional phase, represented by the brittle/ductile ones. Their abutting and crosscutting relationships support this interpretation.

The structural analysis performed on *en-échelon* sedimentary injections perpendicularly cutting the limbs and the crest of a ca. 20 m-sized, substrate olistolith deformed into a large sheath-shaped fold suggests a folding mechanism achieved by an oblique flexural slip-type, layer-parallel shearing (fig. 13). This deformation developed with mechanical contrast of the internal elements (i.e. sandstone-mudstone interbeds) and the outer side of the folded slide block (i.e. olistolith-matrix contact). This evidence, accordingly to the radial distribution of matrix injections around the hinge zones of some rootless folds, suggest a passive folding of rigid/visco-plastic elements (i.e. slide blocks/olistoliths) contained within a progressively deforming liquefied medium (i.e. sedimentary matrix).

Along these injection structures, changes in the grain size of the intruded breccia have been

observed to change in function of the thickness of the injection, with fine-grained portions (i.e. clay-marl) in the narrowest zones and within the cusps, and coarse-grained breccia in the widest ones, suggesting an elutriation process due to forced injection of the matrix, with clogging and consequent mechanical sieving of the finer particles. This evidence supports the interpreted liquid state of the sedimentary matrix.

All of these elements are products of processes that require defined boundary conditions: 1) water-saturated sediment, 2) loose to poorly consolidated material, 3) low-confining stress and 4) high rates of deformations. These conditions are incompatible with a tectonic origin and support the sedimentary nature of the investigated units.

5.2 Paleo-transport directions

Combining all the structural data collected on the U2 of the Vernasso unit a predominant paleo-transport direction toward the N-NE can be outlined, whereas a dominant NNE-directed paleo-transport direction characterizes the U1 of the MB15 (fig. 14). This is in line with the interpretations based on compositional/provenance data of the internal components given by Tunis and Venturini (1992) and Catani and Tunis (2001). In this framework, the mechanical striations found at the base of the marly olistolith of the MB15 are interpreted as tool marks likely caused by the friction of the rigid clasts contained in the basal breccia onto the softer marly material of the slide block (see fig. 7G), and thus possibly related to post-depositional accommodation of the slide block achieved through rotations along its vertical and horizontal axes (see fig. 14D and 16C).

In the Anhovo quarry MTDs, collected structural data suggest overall southerly-directed paleo-transport directions, even if with a quite large spread of azimuths, roughly between N250E and N190E for the Rodež unit, between N200E and N120E for the Perunk 1 unit, and between N190E and N160E for the Perunk 2 unit (fig. 15). On the basis of the main compositions and relative inferred provenances, Skaberne (1987) suggests a source area located to the SE and E for these carbonate MTDs. This discrepancy is likely due to the coeval and similar nature of the sedimentary

deposits rimming the southeastern part of the basin, the proximal depositional environment and the structurally-confined setting (see below).

Other systematic indications of later (post-depositional) deformation of ductile and brittle/ductile discontinuities (e.g. folds' axial planes, shear zones, units' boundaries, matrix injections etc.) can be used as kinematic indicators of the post-emplacement, slide mass accommodation. In this specific case, the downward wedging injections at the base of the U3 appear to be reworked accordingly to a shearing couple roughly coincident with the inferred paleo-transport direction of the underlying U2 (see fig. 15B, E and G).

In the arisen framework, these MTDs seem to originate from two different areas, located in the southern-southwestern sectors for the Vernasso units (i.e. MB 11 and MB15) and in the northern-northeastern sectors for the Anhovo units (Rodež, Perunk 1 and Perunk 2). Accordingly to Tunis and Venturini (1992; 1997) on the NW-SE-directed, elongated and narrow shape of this (inner) foredeep basin, these slide mass could have spread out along the basin coming either from the "passive" (SW) or "active" (NE) margin and then laterally forced along the basin axis (as documented for other exhumed MTDs elsewhere; Ogata, 2010; Ogata *et al*., 2012b), or directly funneled from the opposite sides following the direction of the main sediment delivery systems. In this framework, the investigated examples seem to be located in the SE tip of the elongated foredeep basin, characterized by converging sedimentary inputs (see fig. 3C), with the Vernasso and Anhovo areas in relatively distal and proximal positions, respectively. This interpretation is also supported by the occurrence of erosional unconformities and onlap relationships, and the higher amount of coarse-grained and thick-bedded deposits in the background sedimentary succession of the Anhovo section compared to the Vernasso section. A similar trend is also observed in the Pyreneean counterparts of the Eocene Hecho Group (see among the others Seguret *et al*., 1984; Payros *et al*., 1999), with mass transport events coming from the both sides of the basin. Further work is planned in other localities to implement these interpretations.

5.3 Depositional processes

The inferred process generating the MTDs is that of a bipartite coherent/cohesive flow composed by a lower, debris-blocky flow/avalanche bearing out-sized carbonate and siliciclastic slide blocks (U1 and U2, respectively), overlain by an upper diluted debris/grain-flow (U3). The parent flow can be considered tripartite if the associated upper high- to low-density fully turbulent part (U4 and U5) is taken into consideration (fig. 16A and B). The lower slide division (i.e. U1) represents itself the expression of a bipartite mass flow with a basal, thinner matrix-dominated portion, and an upper, thicker block-dominated portion, also characterized by different types of background sedimentary matrix.

The proposed mechanism of suspension and transport for such deposits is a combination of matrix (sediment+water) overpressure, dispersion pressure due to grain-to-grain interactions and buoyant forces possibly characterizing the less dense enclosed elements respecting to the hyper-concentrated matrix (e.g. vuggy, gas-charged? carbonates, and the loosely-packed/poorly-compacted substrate rip-up blocks).

Such bodies are thought to become highly erosive when the slope gradient breaks and the slide mass "freezes" dissipating the fluid overpressure (e.g. base of the slope-basin plain transition, impact against paleo-topographic highs; Ogata *et al*., 2012a), entraining large portions of loose to poorly-lithified sediments from the seafloor and the underlying sedimentary sequence (fig. 16B).

The emplacement of the lower portion of the slide mass (U1 and U2) is achieved through differential movements of the internal components, with shearing and flowing of the overpressured background matrix, followed by the passive deformation/accommodation of the plastic olistoliths and the underlying sedimentary interval (fig. 16C). The upper portion (U3, U4 and U5) is interpreted to drape the uneven upper surface of the U2 (i.e. block-dominated division) smoothening the asperities and relatively flattening the upper surface of the MTDs (fig. 16A and B).

Mesoscale sedimentary injections into the olistoliths of the U1 and U2 represent a strong evidence of the fluid overpressure developed within the breccia matrix and testify the rheologic contrast

between the plastic slide blocks, and the surrounding matrix (see above). The same structures have been documented by microstructural analyses performed on thin sections, confirming the fluid overpressure-related liquefied state of the injected breccia matrix and the background sedimentary matrix (see fig. 8).

Post-depositional processes further complicate this structural framework, deforming and reworking preceding internal structures. These processes, acting progressively from the deposition to the deep burial, can be summarized in: 1) accommodation, 2) compaction, 3) diagenesis and 4) tectonics. The retention of excess pore pressure within the matrix of a thick, "frozen" slide mass is expected to last quite a long time after the event as confirmed by field-base studies (Strachan, 2002), geophysical investigations (Diviacco *et al*., 2006; Moernaut *et al*., 2009), experiments and numerical modeling (Major, 2000) and it is thus inferred to control early post-depositional processes such as accommodation and compaction.

This is in line with the occurrence of fluid escape structures and shearing at the U2-U3 contact, folded and deformed breccia matrix injections, and folds' interference, which are thought to record later syn-depositional and early post-depositional movements of the entire slide mass. Even if the overall deformation is accommodated by the mutual deformation of the bipartitions, a rheological decoupling located along the U2-U3 contact occurred, testifying slightly different mechanical behaviors between the two. The concordance of these superimposed movements with the paleo-transport directions of the slide events can be thus interpreted a slow-rated, gravity-driven, down-slope accommodation movement (e.g. creeping) of the entire slide mass (see fig. 15B, E and G).

Other lines of evidence can be found in the sedimentary sections lying above the MTDs, in the "channelized" carbonate breccia bodies. Some of them locally form deep scours filled by remolded material similar to the main MTDs' matrix (U2-type) and capped by a relatively tabular and laterally continuous marly layer (U5-type) through a bypass surface (see fig. 12I); accordingly to the paleo-transport directions and the lithologies, these features could be interpreted as up-slope expressions of larger MTDs (comparable to the Rodež, Perunk 1 and Perunk 2 units). In this

framework these deep scours could represent the infilling of slide scars or large-scale grooves caused by the dragging of olistoliths on the seafloor, as documented elsewhere (Draganits *et al*., 2008). Others are located directly above the margins of the main olistoliths, suggesting that the differential compaction between rigid olistoliths and the plastic matrix controls the later deposition for the rest of the cyclothem (see fig. 11B). These stratigraphic intervals expressing the recovery of the "normal", periodic sedimentation above the "impulsive", episodic mass transport events, suggest relatively long-term relationships between mass transport processes and subsequent sedimentation.

The layer-parallel shearing deformation recorded in the sedimentary interval between the Rodež and Podbrdo units (see fig. 12 and 15C) could be interpreted as related to: 1) syn-sedimentary thrust tectonics driven by the approaching of the deformation front from the E to the W (proto-Dinaric fold-and-thrust belt?), 2) gravity driven slope tectonics controlled by the syn-sedimentary uplift of an E-NE structure, 3) mass transport-induced substrate deformation, or 4) slump-type slide mass capsized within its own slide scar (up-slope MTD equivalent?). At the current stage of the research we cannot point out a single interpretation and further work is planned to address these points.

5.4 Possible triggering mechanisms and pre-conditioning factors

Due to the complex interaction of different tectonic contributions in the area (i.e. Alpine and Dinaric) and the particular Paleocene-Eocene environmental context (Miller *et al*., 2005 and reference therein), several types of short- and long-term triggering mechanisms could be invoked as causes for the Paleocene-Eocene carbonate MTDs of the Friuli Basin: 1) seismic shocks, 2) progressive tectonic oversteepening of the leading slopes (both on the external foreland "passive" margin and on the internal "active" margin due to flexural loading and fold-and-thrust belt growth, respectively), 3) long-term variations of the local to regional hydrogeologic regime, 4) first- to second-order sea level changes, etc..

Whereas the classically proposed triggering mechanism is the seismic shock, crucial pre-

conditioning factors could be invoked for the investigated stratigraphic interval, directly or indirectly related to climatic events developed consequently to the roughly coeval Paleocene-Eocene Climatic Transition: 1) storm waves loading-unloading cycles, 2) increased sediment delivery, 3) floods, 4) second- to third-order sea level changes, 5) temporary changes in the local paleo-hydrologic systems, etc. (Katz *et al*., 1999). In this framework, given the occurrence of primary vuggy (gas-charged?) carbonates, slope instabilities related to gas hydrate dissociation could represent another possible working hypothesis for future investigations. Another highly speculative but fascinating possible issue arising from published isotopic analyses concerns the possible relationships of these MTDs with bolide impacts, as already proposed by Marjanac (2000) on the basis of the increased input of cosmic material documented for that period (Kent *et al*, 2003), also in this same area (Dolenec *et al*., 2000).

Further work is planned to integrate the database compiled for the MTDs with detailed stratigraphic and structural analyses from nearby areas in order to compile a comprehensive summary of the geodynamic and paleo-geographic evolution of this sector of the basin.

6. Conclusions

The carbonate “megabreccia” units of the Paleogene Friuli Basin represent fossil examples of large-scale, basin wide MTDs caused by shallow-water carbonate platform collapses sliding from marginal shelfal areas to a relatively deep, evolving inner foredeep basin system of the proto-Dinaric orogen. These catastrophic events generated bipartite, fast moving slide masses composed of a lower cohesive, blocky/debris flow part with olistoliths exceeding 100 m across and an upper turbulent flow, able to deeply erode the overridden seafloor incorporating large amounts of ripped off material. During their downslope motion, internal and basal friction forces were dissipated by fluid overpressure conditions provided by the undrained, fine-grained matrix, allowing the slide mass to accelerate and move fast until it reaches the slope-basin plain transition.

Meso-scale structural, stratigraphic and sedimentologic data were collected to identify mass

transport-related mechanisms of deformation, depositional processes and paleo-transport directions of four of the largest MTDs in the Vernasso (Italy) and Anhovo (Slovenia) quarries. Ductile and ductile/brittle structures such as rootless folds, plastic shear zones and matrix injections are interpreted to record syn- to early-post depositional phases of the slide mass evolution, testifying the crucial role of a liquefied, overpressured sedimentary matrix in the accommodation of the high-rated internal strain. Such MTDs are also thought to influence the host sedimentary succession through deep erosion and deformation of the substratum, post-depositional accommodation and consequent control on the overlying "normal", background sedimentation with the creation of seafloor topography.

In the paleogeographic framework that arises from the inherent literature, the differences found between the two study sites in terms of paleo-transport directions and background sedimentary successions preliminarily suggest that these MTDs were likely emplaced in different depocenters belonging to the same basin complex (i.e. lateral closure of the inner foredeep) and fed by different source areas rimming the basin margins. In this context the Vernasso area occupies a relatively distal position compared to the Anhovo area with respect to the source areas located to the western and eastern margins of the foredeep basin, respectively. In such confined physiographic situation, converging pathways of sedimentary transport coming from shallow-water areas are expected to consequently steer along the basin axis, roughly toward the NW (see fig. 3C).

Concluding, as arises from an updated review of the modern marine geology database, a correct understanding of the generating processes of these MTDs, achievable only through integrated studies with direct, detailed observations on ancient analogues, is for example crucial to estimate the socio-economic risk linked to submarine landslide-related geohazards.

Acknowledgments

We would like to thank David J. Piper and two anonymous reviewers for having greatly improved the quality of the manuscript with their suggestions and criticism. The Salonit Anhovo Co. and Dr.

Stefano Piccini are also gratefully acknowledged for having allowed this study.

References

Alonso, J.L., Marcos, A., Suárez, A., 2006. Structure and organization of the Porma mélange: progressive denudation of a submarine nappe toe by gravitational collapse. American Journal of Science 306, 32-65.

Alves, T., Lourenco, S. 2010. Geomorphologic features related to gravitational collapse: submarine landsliding to lateral spreading on a Late Miocene-Quaternary slope (SE Crete, eastern Mediterranean). Geomorphology 123, 13-33.

Arnaud, E., Eyles C.H., 2002. Catastrophic mass failure of a Neoproterozoic glacially influenced continental margin, the Great Breccia, Port Askaig Formation, Scotland. Sedimentary Geology 151, 313–333.

Bigi, G., Cosentino D., Parotto M., Sartori R., Scandone P., 1990. Structural Model of Italy, 1:250.000. CNR and SELCA.

Bradley, D., Hanson, L., 1998. Paleoslope Analysis of Slump Folds in the Devonian Flysch of Maine. Journal of Geology 106, 305–318.

Burg, J.P., Bernoulli, D., Smit, J., Dolati, A., Bahroudi, A., 2008. A giant catastrophic mud and debris flow in the Miocene Makran. Terra Nova 20, 181–193.

Buser, S. 1987. Osnovna geološka karta SFRJ, list Tolmin in Videm, L33-64 1:100.000 = Geological map of SFRJ 1: 100.000, sheet Tolmin and Udine. Zvezni geološki zavod, Beograd.

Callot, P., Sempere, T., Odonne, F., Robert, E., 2008a. Giant submarine collapse of a carbonate platform at the Turonian-Coniacian transition: The Ayabacas Formation, southern Peru. Basin Research 20, 333–357.

Callot, P., Odonne, F., Sempere, T., 2008b. Liquification and soft-sediment deformation in a

limestone megabreccia: the Ayabacas giant collapse, Cretaceous, southern Peru. Sedimentary Geology 212, 49–69.

Cati, A., Sartorio D., Venturini S., 1987. Carbonate platforms in the subsurface of the northern Adriatic area. Mem. Soc. Geol. It. 40, 295-308.

Catani, G., Tunis, G., 2001. Caratteristiche sedimentologiche dei megabanchi carbonatici paleogenici del Bacino Giulio (Valli del Natisone, Friuli orientale). Studi Trentini di Scienze Naturali Acta Geologica 77, 81-102.

Carulli, G.B., 2006. Carta Geologica del Friuli Venezia Giulia. Ed. Regione Autonoma Friuli Venezia Giulia, Direzione Centrale Ambiente e Lavori Pubblici, Servizio Geologico.

Codegone, G., Festa, A., Dilek, Y., Pini, G.A., 2012. Small-scale polygenic mélanges in the Ligurian accretionary complex, Northern Apennines, Italy, and the role of shale diapirism in superposed mélange evolution in orogenic belts. Tectonophysics 568-569, 170-184.

Csontos, L., Vörös, A., 2004. Mesozoic plate tectonic reconstruction of the Carpathian region. Paleogeography Paleoclimatology Paleoecology 210, 1–56.

De Capoa, P., Radoicic, R., 2002. Geological implications of biostratigraphic studies in the external and internal domains of the Central-Southern Dinarides. Mem. Soc. Geol. It. 57, 185-191.

Debacker, T.N., Dumon, M., Matthys, A., 2009a. Interpreting fold and fault geometries from within the lateral to oblique parts of slumps: A case study from the Anglo-Brabant Deformation Belt (Belgium). Journal of Structural Geology 31, 1525–1539.

Debacker, T.N., De Meester, E. 2009b. A regional, S-dipping late early to middle Ordovician paleoslope in the Brabant Massif, as indicated by slump folds (Anglo-Brabant Deformation Belt, Belgium). Geologica Belgica 12/3-4, 145-159.

Diviacco, P., Rebesco, M., Camerlenghi, A., 2006. Late Pliocene mega debris flow deposit and related fluid escapes identified on the Antarctic Peninsula continental margin by seismic reflection data analysis. Marine Geophysical Research 27, 109–128.

Dolenec, T., Pavšič, J., Lojen, S. 2000. The Paleocene-Eocene boundary in a flysch sequence from

Goriška Brda (Western Slovenia): Oxygen and carbon stable isotope variations = Paleocensko-eocenska meja v flišu Goriških Brd (zahodna Slovenija): variabilnost izotopske sestave kisika in ogljika. Geologija 43/1, 37-42.

Draganits, E., Schlaf, J., Grasemann, B., Argles, T., 2008. Giant submarine landslide grooves in the Neoproterozoic/Lower Cambrian Phe Formation, northwest Himalaya: mechanisms of formation and paleogeographic implications. Sedimentary Geology 205, 126–141.

Feruglio, E. 1925. Carta geologica delle Tre Venezie.Foglio 25, Udine. Ufficio Idrografico R. Magist. Acque Venezia. Firenze.

Gnaccolini, M., 1968. Sull'origine del "conglomerate pseudo-cretaceo" di Vernasso (Cividale del Friuli). Riv. Ital. Paleont. 74, 1233-1254.

Johns, D.R., Mutti, E., Rosell J., Seguret M., 1981. Origin of a thick redeposited carbonate bed in the Eocene turbidites of the Hecho Group, south central Pyrenees, Spain. Geology 9, 161-164.

Hansen, E., 1971. Strain Facies. Springer-Verlag, Berlin, 207 pp.

Katz, M.E., Pak, D.K., Dickens, G.R., Miller, K.G., 1999. The Source and Fate of Massive Carbon Input During the Latest Paleocene Thermal Maximum. Science 286, 1531-1533.

Kent, D.V. Cramer, B.S., Lanci, L., Wang, D., Wright, J.D., Van der Voo, R., 2003. A case for a comet impact trigger for the Paleocene/Eocene thermal maximum and carbon isotope excursion. Earth and Planetary Science Letters 211, 13-26.

Kušcer, D., Grad, K., Nosan, A., Ogorelec, B., 1974. Geološke raziskave soške doline med Bovcem in Kobarid (Geology of the Soca Valley between Bovec and Kobarid). Geologija 17, 425-476.

Labaume, P., 1992. Evolution tectonique et sédimentaire des front de chaîne sous-marins. Exemples des Apennins du Nord, des Alpes françaises et de Sicile. unpublished PhD thesis, University of Montpellier; 476 pp..

Lucente, C.C., Pini, G.A., 2003. Anatomy and emplacement mechanism of a large submarine slide within a Miocene foredeep in the Northern Appennines, Italy: a field perspective. American Journal of Science 303, 565-602.

Lucente, C.C., Pini, G.A., 2008. Basin-wide mass-wasting complexes as markers of the Oligo-Miocene foredeep-accretionary wedge evolution in the Northern Apennines, Italy. Basin Research 20, 49 – 71.

Macdonald, D.I.M, Moncrieff, A.C.M., Butterworth, P.J., 1993. Giant slide deposits from a Mesozoic fore-arc basin, Alexander Island, Antarctica. Geology 21/11, 1047-1050.

Major, J.J., 2000. Gravity-driven consolidation of granular slurries: implications for debris-flow deposition and deposit characteristics. Journal of Sedimentary Research 70/1, 64-83.

Marjanac, T., 1996. Deposition of megabeds (megaturbidites) and sea-level change in a proximal part of the Eocene-Miocene flysch of central Dalmatia (Croatia). Geology 24/6, 543-546.

Marjanac, T., 2000. Giant beds - impact induced deep-marine deposits. Abstracts Catastrophic events & mass extinctions: Impacts and beyond. Vienna 2000. LPI Contribution No. 1053, 125-126

Melosh, J.H., 1987. The mechanics of large rock avalanches. GSA Rev. in Engineering Geology 7, 41-49.

Merlini, S., Doglioni, C., Fantoni, R., Ponton, M., 2002. Analisi strutturale lungo un profilo geologico tra la linea Fella-Sava e l'avampaese adriatico (Friuli Venezia Giulia-Italia). Mem. Soc. Geol. It. (Roma) 57, 293–300.

Middleton, G.V., Hampton, M.A., 1973. Sediment gravity flows: mechanics of flow and deposition. In: G.V. Middleton, A.H. Bouma (Eds.), Turbidites and Deep-water Sedimentation, SEPM Pacific Section, Short Course Notes, 1-38.

Miller, K.G., Kominz, M.A., Browning, J.V., Wright, J.D., Mountain, G.S., Katz, M.E., Sugarman, P.J., Cramer, B.S., Christie-Blick, N., Pekar, S.F., 2005. The Phanerozoic record of global sea-level change. Science 310, 1293-1298.

Moernaut, J., De Batist, M., Heirman, K., Van Daele, M., Pino, M., Bru□mmer, R., Urrutia, R., 2009. Fluidization of buried mass-wasting deposits in lake sediments and its relevance for paleoseismology: results from a reflection seismic study of lakes Villarrica and Calafquén

(South-Central Chile). Sedimentary Geology 213, 121–135.

Mutti, E., 1992. Turbidite Sandstones. San Donato Milanese, Agip-Istituto di Geologia, Università di Parma, 275 pp.

Mutti, E., Carminatti, M., Moreira, J.L.P., Grassi, A.A., 2006. Chaotic Deposits: examples from the Brazilian offshore and from outcrop studies in the Spanish Pyrenees and Northern Apennines, Italy. A.A.P.G. Annual Meeting, April 9-12, Houston, Texas.

Ogata, K., 2010. Mass transport complexes in structurally-controlled basins: the Epiligurian Specchio Unit (Northern Apennines, Italy). Unpublished PhD thesis, University of Parma.

Ogata, K., Mutti, E., Pini G.A., Tinterri, R., 2012a. Mass transport-related stratal disruption within sedimentary mélanges. Tectonophysics 568-569, 185-199.

Ogata, K., Tinterri, R., Pini, G.A., Mutti, E., 2012b. The Specchio Unit (Northern Apennines, Italy): an ancient mass transport complex originated from near-coastal areas in an intra-slope setting. In: Y. Yamada, K. Kawamura, K. Ikehara, Y. Ogawa, R. Urgeles, D. Mosher, J. Chaytor, M. Strasser (Eds.), Submarine Mass Movements and Their Consequences. Advances in Natural and Technological Hazards Research. Springer Netherlands, 595-605.

Passchier, C.W., Trouw, R.A., 2005. Microtectonics. Springer Berlin Heidelberg New York. 365.

Payros, A., Pujalte, V., Etxebarria, X.O., 1999. The South Pyrenean Eocene carbonate megabreccias revisited: new interpretation based on evidence from the Palmona Basin. Sedimentary Geology 125, 165–194.

Perricone, L., 2003. Osservazioni sedimentologiche per la ricostruzione paleogeografica del settore paleocenico ed eocenico delle Valli del Natisone. Harmonia, 1, 55-94.

Phillips, E.R., 2006. Micromorphology of a debris flow deposit: evidence of basal shearing, hydrofracturing, liquefaction and rotational deformation during emplacement. Quaternary Science Reviews 25, 720–738.

Piccoli, G., Proto Decima, F., 1969. Ricerche biostratigrafiche sui depositi flyschoidi della regione Adriatica settentrionale e orientale. Mem. Istituti di Geologia e Mineralogia dell'Università di

Padova 27, 3-21.

Pini, G.A., 1999. Tectonosomes and olistostromes in the Argille Scagliose of the Northern Apennines, Italy. Geol. Soc. of America Special Publ. 335, 73 pp..

Pini, G.A., Ogata, K., Camerlenghi, A., Festa, A., Lucente, C.C., Codegone, G., 2012. Sedimentary mélanges and fossil mass-transport complexes: a key for better under- standing submarine mass movements? In: Y. Yamada, K. Kawamura, K. Ikehara, Y. Ogawa, R. Urgeles, D. Mosher, J. Chaytor, M. Strasser (Eds.), Submarine Mass Movements and Their Consequences. Advances in Natural and Technological Hazards Research. Springer Netherlands, 585-594.

Pirini, C., Tunis, G. e Venturini, S., 1986. Biostratigrafia e paleogeografia dell' area sud-occidentale del M. Mia-M. Mataiur (Prealpi Giulie). Riv. Ital. Paleont. Strat. 92 (3), 327-382.

Placer, L., 1981. Geološka zgradba jugozahodne Slovenije = Geologic structure of southwestern Slovenia. Geologija 24/1, 27—60

Placer, L., 1998. Contribution to macrotectonic subdivision of the border region between Southern Alps and External Dinarides = Prispevek k makrotektonski rajonizaciji mejnega ozemlja med Južnimi Alpami in Zunanjimi Dinaridi. Geologija 41, 223-255.

Placer, L., Vrabec, M., Celarc, B., 2010. The bases for understanding of the NW Dinarides and Istria Peninsula tectonics = Osnove razumevanja tektonske zgradbe NW Dinaridov in polotoka Istre. Geologija 53/1, 55-86.

Pogačnik, Ž., 2010. Interpretacija geoelektrične anomalije v krovnini cikloteme Perunk-zgornje paleocenski fliš kompleks okolice Anhovega = Interpretation of geoelectric anomalies in the terminal part of Perunk cyclotheme-upper Paleocene flysch deposits near Anhovo. In: Košir, A., Horvat, A., Zupan Hajna, N., Otoničar, B., (Eds.), Abstracts and excursions, 3rd Slovenian Geological Congress, ZRC SAZU, 111 str., Ljubljana.

Pogačnik, Ž., Pavšič, J., Meden, A., 2009. The geological record as an indicator of the mudstones thermal characteristics in the temperature range of decarbonatisation = Geološki zapis kot

pokazatelj termičnih lastnosti laporovcev v temperaturnem območju dekarbonatizacije. Mater. Technol. 43/3, 157-163.

Pogačnik, Ž., Stupar, M., 2006. The extraction of raw materials for the cement industry and nature conservation = Zagotavljanje primernih materialov za cementno industrijo s ciljem ohranjanja narave. Mater. Technol. 40/4, 139-143.

Ponton, M., Turco, S., 1997. La Grotta di San Giovanni d'Antro. Geologia dell'area ed evoluzione della cavità. In Muscio G. (Eds), Il fenomeno carsico delle Valli del Natisone (Prealpi Giulie). Mem. Istit. Ital. di Spel., s. II, 9: 119-126, Udine.

Rožič, B., Šmuc, A.,2011. Gravity flow deposits in the Toarcian Perbla Formation (Slovenian Basin, NW Slovenia). Rivista Italiana di Paleontologia e Stratigrafia 117, 283-294.

Sartorio, D., Tunis, G., Venturini, S., 1987. Il pozzo SPAN 1: nuovi contributi per l' interpretazione geologica e paleogeografica delle Prealpi Giulie (Friuli orientale). Riv. It. Paleont. Strat. 93 (2), 181-200.

Seguret, M., Labaume, P. Madariaga, R., 1984. Eocene seismicity in the Pyrenees from megaturbidites on the South Pyrenean Basin, Spain. Mar. Geol, 55, 117-131.

Selli, R., 1953. La geologia dell'alto bacino dell'Isonzo. Giorn. Geol. Bologna 2/19, 1-153.

Skaberne, D., 1987. Megaturbidites in the Paleogene Flysch in the region of Anhovo (W Slovenia, Yugoslavia). Mem. Soc. Geol. It. 40, 231-239.

Šmuc, A., 2005. Jurassic and Cretaceous Stratigraphy and Sedimentary Evolution of the Julian Alps, NW Slovenia. Založba ZRC Publishing, Ljubljana, Slovenia, 98 p.

Spence, G.H., Tucker , M.E., 1997. Genesis of limestone megabreccias and their significance in carbonate sequence stratigraphic models: a review. Sedimentary Geology 112, 163-193.

Strachan, L.J., 2002. Slump-initiated and controlled syn-depositional sandstone remobilization: an example from the Namurian of County Clare, Ireland. Sedimentology 49, 25-41.

Strachan, L.J., Alsop, G.I., 2006. Slump folds as estimators of paleoslope: a case study from the Fisherstreet Slump of County Clare, Ireland. Basin Research 18, 451-470.

Tunis, G., Pirini Radrizzani, C., 1987. Flyschoid deposits of Goriška Brda (Collio) between Soča (Isonzo) River and Idrija (Iudrio) River – facies and paleoenvironments. Geologija 30, 123-148.

Tunis, G., Venturini, S., 1992. Evolution of the Southern Margin of the Julian Basin with emphasis on the megabeds and turbidites sequence of the Southern Julian Alps (NE Italy). Geologia Croatica 45, 127-150.

Tunis, G., Venturini, S., 1997. La Geologia delle Valli del Natisone. Memorie dell'Istituto Italiano di Speleologia "Il fenomeno carsico delle Valli del Natisone" 9/2, 35-48.

Van der Merwe, W.C., Hodgson, D.M., Flint, S.S., 2009. Widespread syn-sedimentary de-formation on a muddy deep-water basin-floor: the Vischkuil Formation (Permian), Karoo Basin, South Africa. Basin Research 21, 389–406.

Venturini, S., Tunis, G., 1992. La composizione dei conglomerati cenozoici del Friuli: dati preliminari. St. Geol. Camerti, vol. sp. (1992/2), CROP 1-1A, 285-295.

Venzo, G.A., Brambati, A., 1969. Prime osservazioni sedimentologiche sul Flysch Friulano. St. Trent. Sc. Nat. sez. A; 46/1, 3-10.

Weimer, P., 1989. Sequence stratigraphy of the Mississippi Fan (Plio-Pleistocene), Gulf of Mexico. Geo-Marine Letters 9, 185-272.

Woodcock, N.H., 1979. The use of slump structures as paleoslope orientation estimators. Sedimentology 26/1, 83 – 99.

Yamamoto, Y., Nidaira, M., Ohta, Y., Ogawa, Y., 2009. Formation of chaotic rock units during primary accretion processes: examples from the Miura-Boso accretionary complex, central Japan. The Island Arc 18, 496-512.

Zanferrari, A., Avigliano, R., Carraro, F., Grandesso, P., Monegato, G., Paiero, G., Poli, M.E., Rogledi, S., Toffolon, G., Tunis, G., 2008. Geological map and explanatory notes of the Italian Geological Map at the scale 1:50.000: Sheet 066 "Udine". APAT-Servizio Geologico d'Italia – Regione Autonoma Friuli Venezia Giulia.

http://www.isprambiente.gov.it/Media/carg/friuli.html.

Zanferrari, A., Masetti, D., Monegato, G., Poli, M.E., 2013. Geological map and explanatory notes of the Italian Geological Map at the scale 1:50.000: Sheet 049 "Gemona del Friuli". ISPRA - Servizio Geologico d'Italia - Regione Autonoma Friuli Venezia Giulia, 262 pp. http://www.isprambiente.gov.it/Media/carg/friuli.html.

Zuffa, G.G., 1980. Hybrid arenites: their composition and classification. Journal of Sedimentary Petrology 50, 21-29.

Figure captions

Figure 1. Simplified geological map of the Dinarides-Southern Alps junction with location of the investigated areas. Main sources: Bigi et al., 1990 and Placer *et al*., 2010.

Figure 2. A: Geologic map of the Julian Pre-Alps of the Eastern Friuli and Western Slovenia. The circled numbers refer to the stratigraphic logs of fig. 3. Compiled after Catani and Tunis (2001) and Buser (1987). B: Schematic stratigraphic column of the upper Campanian-Paleogene clastic deposits of the Julian Basin (redrawn and modified from Catani and Tunis (2001) and Buser (1987).

Figure 3. A: Correlation of megabeds in the Friuli Basin (datum in the schematic stratigraphic logs = top of MB11, thickness maintained). Locations of sections are in fig. 2. Redrawn and modified from Tunis and Venturini (1992). The five depositional units are defined from Tunis and Venturini (1992). B: Conceptual cartoon showing the main internal subdivisions of the "megabreccia" bodies (see text for explanation). Modified from Seguret *et al*. (1984). C: Paleogeographic map of the Friuli Basin at the early Ypresian (Ilerdian), from Pirini *et al*., 1986, redrawn and modified. The map is based on the present day position of the stratigraphic

sections and outcrops (see A and fig. 2A), with no retro-deformation of tectonic structures (i.e. not a palinspastic reconstruction).

Fig. 4. Summary of the ductile deformation-related kinematic indicators used in this work with identification of the collected structural parameters: 1) asymmetric boudinage, 2) pseudo-Sigma and 3) pseudo-SC (i.e. ”shear/cleavage”) and duplex/imbrication structures, 4) intrafolial, hydroplastic and drag folds, and 5) pseudo-deformation/disaggregation bands, and 6) mechanical lithologic mixing.

Fig. 5. Vernasso quarry case study. A: Aerial photograph of the Vernasso quarry (Google Earth Pro, 2013) showing the points of view of photographs in B and C. B: Mixed siliciclastic carbonate turbidites with intercalated smaller megabeds (MB12 and MB13) cropping out atop megabed 11 (MB11). C: Overview of the Vernasso quarry looking toward the W. The megabeds (MB11-MB15), their internal subdivisions (depositional units: U1 to U5), and the locations of the structural stations (1 to 7) are labeled. D, E: Upper part of the Unit 2 (U2) of MB11 (locations in fig. 4C): dashed line marks the boundary with the Unit 3 (U3) and solid lines outline the blocks of intrabasinal sediments (rip-up substrate blocks). Frames refer to pictures in fig. 5. F: Schematic stratigraphic log of the Vernasso quarry section. The background lithologies (mixed siliciclastic-carbonate turbidites) are marked in green and the depositional units of megabeds are distinguished (UI to U5). Modified from Catani and Tunis (2001).

Fig. 6. Ductile and brittle thrusts, and sedimentary injections in the U2 of the Vernasso unit (MB11). A, B, C, D and E: Examples of breccia injections within rip-up substrate blocks, white lines outline the matrix-block boundaries. Location of A and B are in Figs. 4D and 5E, locations of C and D are in fig. 6B and 6C, respectively. F, G, H and I: Examples of ductile (D-type; yellow) and brittle (B-type; red) shear zones. The sense of movement of the hangingwall and

the relative timing (1 older, 2 younger) are labeled. White solid lines mark the edges of substrate blocks; dash-dot lines in I highlight bed surfaces. Locations of G and I are in fig. 5E and 5G, respectively.

Fig. 7. Meso-scale structures in the U1 of the Porzus unit (MB15). A: Basal contact (thick, dotted white line) of the MB15 and substrate sediments deformations (structural station 7 in fig. 5C). B, C, D and E: Photomontages/photographs of southern (B, C) and northern (D, E) parts of the exposure (location in A). Solid white lines and thin dotted lines border the blocks (olistoliths) and the different types of matrix, respectively. Low angle ductile shear zones (yellow) deform the thin-bedded turbidites and are offset by brittle faults (red). Symbols as in Figs. 6F-I. Below the main basal olistolith, from the left (S) to the right (N) of photomontage D, the ductile shear zones changes from normal to reverse motion, because of their listric, concave shape. F: Close up of E showing an imbricate system of small-offset, reverse shear zones and the related soft sediment (mesoscopic ductile) folding. G: Mechanical striations without evidence of calcite growth recognizable at the base of the main marly olistolith (location shown in D).

Fig. 8. Injected and basal sedimentary matrix of the Vernasso (MB11) and Porzus (MB15) units, respectively. A, B: Thin section microphotographs (left) and interpretations (right) of the breccia matrix that constitutes a bended injection in a marly olistolith (location in fig. 6E). C, D: Thin section microphotographs of the basal breccia immediately below the main marly olistolith of fig. 7G. Thin sections are oriented accordingly to the strike and dip of the lenticular breccia layer, respectively. Bed polarity (i.e. stratigraphic up), scale bar and sample ID are labeled.

Fig. 9. Anhovo quarry case study. A: Aerial photograph of the Anhovo quarry (Google Earth Pro,

2013). B: Main sedimentary bodies in the SE side of the Perunk quarry sector (photograph taken from B in A). C: Main sedimentary bodies and the internal subdivisions (depositional units U1 to U5) of Rodež unit (photograph taken from C in A) in the Rodež quarry sector. The white boxes (1 to 3) represent the approximate extent of the measurement stations. D: Large meso-scale sheath-type fold showing an arcuate axis (dashed line). Location in C. E: Radial distribution of U3 breccia matrix injections (white arrows) around a folded rip-up olistolith belonging to the underlying U2 (Rodež unit, location in C). F: Schematic stratigraphic log of the Anhovo quarry section. The internal depositional units (U1 to U5) of megabeds are represented. The background lithologies (mixed siliciclastic-carbonate turbidites) are marked in green.

Fig. 10. Meso-scale structures in the U2 of the Rodez and Perunk units. A: Rip-up olistolith at the U2-U3 boundary within the Perunk 1 unit (NE side of the Perunk quarry sector) deformed in an isoclinal, recumbent syncline with parasitic, intrafolial folds in the hinge zone. The white arrows indicate stratigraphic younging (i.e. depositional up). A sub-horizontal shear zone characterized by abundant breccia matrix is characterized by an intrafolial disarticulation of the fold axial zone (dashed lines bounding yellow transparent overlay cuts the core zone). The overturned upper limb of the olistoliths is intruded by roughly systematic sets (see stereonets of fig. 15) of low- to high-angle cuspidate injections from the overlying rudite of the U3. Circled yellow field notebook for scale. B: Shear zone below the sheared breccia cutting the isoclinally folded block (location in A). Shear-type planes (dashed lines marked with “S”) and subordinate cleavage/foliation-type surfaces (dotted lines marked with “C”) define pseudo-SC shear structures used as kinematic indicators. C: Wedge-shaped sedimentary injections (dashed lines) of the U3 matrix into the upper part of a marly olistolith of the underlying U2. Location in A. D: Detail of a sheath folded block within the U2 of the Rodež unit (location in fig. 9C) pervasively injected in the flanks and the fold core by sedimentary breccia (yellow

transparent overlay). In addition, the sandstone beds (blue transparent overlay) have been liquified and boudinated by a previous deformation event crosscut by the sedimentary injections. Lens cap for scale. E: Sigmoid-shaped, shaly olistoliths characterizing the U2 subdivision of the Perunk 1 unit roughly defining a top-toward-the-right shear zone. F: Pseudo-SC shears and sigmoidal marly intraclast (yellow transparent overlay) in a shear zone at the base of a marly olistolith. The shear zone and the olistolith are deformed by a minor thrust to the right (red dashed line). G: U2-U3 contact within the Rodež unit (location shown in fig. 9C), deformed by a diapir-like, dome-shaped upward intrusion of the U2 "block-in-matrix" material into the overlying carbonate breccia of the U3. Evidence of later tectonic deformation is given by striated shear planes (recognizable whitish, shiny surfaces in the U2), calcite veins, systematic fracture sets and meso-scale faults, usually reworking previously formed discontinuities. Note for instance the meso-scale fracture zone (red dashed line) shown in the picture is roughly coincident with the sidewalls of a sharp sub-vertical injection. Location in fig. 9C. Circled Ž. Pogačnik for scale. See fig. 4 for a summary of the discussed structures.

Figure 11. Meso-scale structures of the Perunk 2 unit. A: Conceptual stratigraphic log and explanation of the Perunk quarry segment section (upper log) and detailed log of the Perunk 2 unit with indication of the internal subdivisions (lower log). B: Overview of the Perunk 2 unit and the host sedimentary succession with labeling of the main elements (transparent overlays; see explanation in A) and the lower and upper contact of the U1-U2 interval (red dashed and solid lines). Approximate position shown in the red box in A. C: Upper middle part of the Perunk 2 unit with indication of the internal subdivisions (see fig. 3B). Location shown in B (black box) and A (small red box). D: Right side margin of the carbonate olistolith. See explanation in A for the labels. Position indicated in A and B. E: Close-up of D showing the "squeezed" matrix and folded substrate sediments at the margin of the slide block. F: Basal,

upward matrix injection into the olistolith (location shown in B). G: Plane view of the matrix injections (same as shown in F) cutting the basal surface of the olistolith. Note their ellipsoidal shape evidencing pipe-like structures in three-dimensions (location shown in B). H: Close up of E showing the appearance of the sedimentary breccia matrix of the U2. I: Polished section of the basal sedimentary breccia showing its matrix-supported texture and the included sub-rounded to sub-angular carbonate clasts (sample position indicated in D and in the lower log represented in A). J: Polished section of the sedimentary breccia matrix shown in H (sample position indicated in F and in the lower log represented in A).

Fig. 12. Meso-scale structures in the background sedimentary succession. A: SE side of the Anhovo quarry (Rodež sector) showing the stratigraphic interval between the upper and lower contacts (white dashed lines) of the Rodež and Podbrdo units. White, yellow and orange overlays highlight three carbonate megabeds. Note the lenticular trend of the megabeds with rapid lateral pinch-outs and channelized parts (see I), and the deep basal scouring of the Podbrdo unit from the left (NE) to the right (SW). On the upper left-hand side also the base of the Perunk 1 unit is exposed, down cutting the substratum and causing the amalgamation with the underlying Podbrdo unit. B, C, D: Branching thrusts (red lines and arrows) affecting the sedimentary interval just above the upper contact of the Rodež unit. Location shown in A. E: Multi-horses, duplex originated from a branching, layer-parallel shear zone developing within laminated shales in between two through-going thrusts. Circled lens cap for scale. F, G: Close up of the lower through-going, branching thrust depicted in D showing bed duplications and minor backthrusting. Lens cap and field notebook for scale. H: Detail of the uppermost through-going thrust (about 10 m below the basal contact of the Podbrdo unit) cutting the channelized carbonate debris flow (orange transparent overlay in A). See A for location. I: Middle megabed (yellow transparent overlay). The unit form a scour into the substrate,

defining a steep-sided channel filled with intraclastic breccia and sharply topped (contact/bypass surface labeled with a white dashed line) by a carbonate turbidite-type bed that thins out laterally over short distance, but maintaining continuity at the whole outcrop scale (see A). Circled Ž. Pogačnik for scale.

Fig. 13. Example of structural analyses performed on a sheath-like folded olistolith. A: Meters to tens of meters-sized rip-up olistoliths floating in a brecciated matrix, U2 subdivision in the Rodež unit (location in fig. 9C). The stereonet (equal area, lower hemisphere) represents the poles to the bedding planes of the large antiformal slide block in the middle of the picture (circled Ž. Pogačnik for scale). B: The outer hinge zone of the antiformal slide block (location in A) presents minor thrust (red dashed line and arrow) and shear plane (white dashed line) and two crosscutting sets of cuspidate sedimentary dykes (white transparent overlays) injecting the sandstone of an overlaying bed within a shaly interval. Circled lens cap for scale. Structural data are represented in the stereonet (equal area, lower hemisphere, planes as great circles): red line for the thrust (shear planes) and black lines for the injections (long axial planes). C, D: Right and left limbs of the antiformal fold of B. The same downward sandy sedimentary injections (white transparent overlays) in the shale interval are arranged in *en-echélon* patterns consistent with an opposite layer-parallel shear (white arrows) in the two limbs. This is in line with flexural-slip deformation in the limbs and inner/outer arc compression/distension during folding. Hammer for scale. The relative stereonets show the attitude of the injections (equal area, lower hemisphere, great circles).

Fig. 14. Results of the structural stations measured at the Vernasso quarry. Data back-tilted to the horizontal. A: Stereonet of ductile folds axes (trend/plunge) subdivided on the basis of their verging direction in Z- (dextral) and S-type (sinistral), plotted accordingly to the separation-arc method proposed by Bradley and Hanson (1998). The data dispersion can be attributed to

the highly curvilinear fold axes (i.e. sheath folds). B: Stereonet of bedding planes within olistoliths. Due to their bedding-related, oblate ellipsoidal shape, bedding coincides with the general disposition of the olistoliths. C: Stereonet of the ductile (D-type) and brittle (B-type) shear surfaces. Locally, the NE-dipping B-type shears are SW-verging thrusts reworking preceding low-angle normal, ductile faults with nearly opposite shearing sense, and vice versa. See text for extended discussion. D: Rose diagram showing the directions of the tool marks (fig. 7G) created by small rigid clasts scratching the base of a marly olistolith. On the basis of the crosscutting relationships, the NNE-SSW directed set is interpreted as syn-depositional (in agreement with the other kinematic indicators), while the WNW-ESE directed set is attributable to late syn-/early post-depositional phases. See text for extended discussion.

Fig. 15. Results of the structural stations measured at the Anhovo quarry. Data back-tilted to the horizontal. A. Paleo-transport directions of the Rodež unit (U2) as inferred from ductile folds axes subdivided into Z- (dextral) and S-type (sinistral) depending on their vergence, and plotted accordingly to the separation-arc method proposed by Bradley and Hanson (1998). In addition, also data on sheath folds and double vergent folds have been plotted as lines (i.e. long axis azimuth). B: Stereonet with representation of the ductile and brittle shear zones, and injections within the Rodež unit (U2). The three clusters are roughly coherent with the transport directions inferred from A. C: Stereonet of thrust surfaces, horses of duplex and pseudo-sigmoidal structures (poles to planes) collected within the “normal” background sedimentary interval between the Rodež and Podbrdo units (see fig. 13A-H). The fairly constrained clustering, roughly coherent with the stereonets shown in A and B, suggest an overall transport direction toward the SW. D: Paleo-transport directions of the Perunk 2 unit (U1-U2) as inferred from ductile folds axes (trend/plunge; see A for explanation). E: Spatial arrangement of the sedimentary injections (axial planes) into the main carbonates olistolith of the Perunk 2 unit. Two main high- and low-angle sets trending approximately perpendicular

and parallel to the paleo-transport direction, respectively, characterize the outer portions of the slide block. F: Stereonet showing the ductile folds' axes collected within the Perunk 1 unit (U2). See A for explanation. G: Syn-sedimentary thrusts, sedimentary injections and main axial plane of sigmoidal elements collected within the olistolith shown in fig. 10A and plotted planes poles to. Resultant cluster are approximately coherent with the preceding (see B and E).

Fig. 16. A: Conceptual evolutionary scheme for the different phases of the slide mass, from acceleration to deposition, with emphasis on dynamic loading-related substrate erosion/bypass. B: Hypothetical close up sketch depicting the mass transport-related erosion of the seafloor, and the internal and the shallow- and deep-substrate deformation features. C: Schematic block diagram showing the brittle/ductile structures and the accommodation deformation patterns of the substrate sediments in response to syn-emplacement/early-post depositional seafloor dragging, and rotations of basal olistoliths.

Highlights

- Vertical slide body partition into basal cohesive and upper turbulent flows;
- Basal subdivision into lower visco-fluid and upper visco-plastic parts;
- Supporting sedimentary matrix with fluid overpressure-related liquefaction;
- Slope-gradient breaks leading to deformation and erosion of the substrate;
- Different source areas and paleo-transport direction for the main MTDs;

Figure1

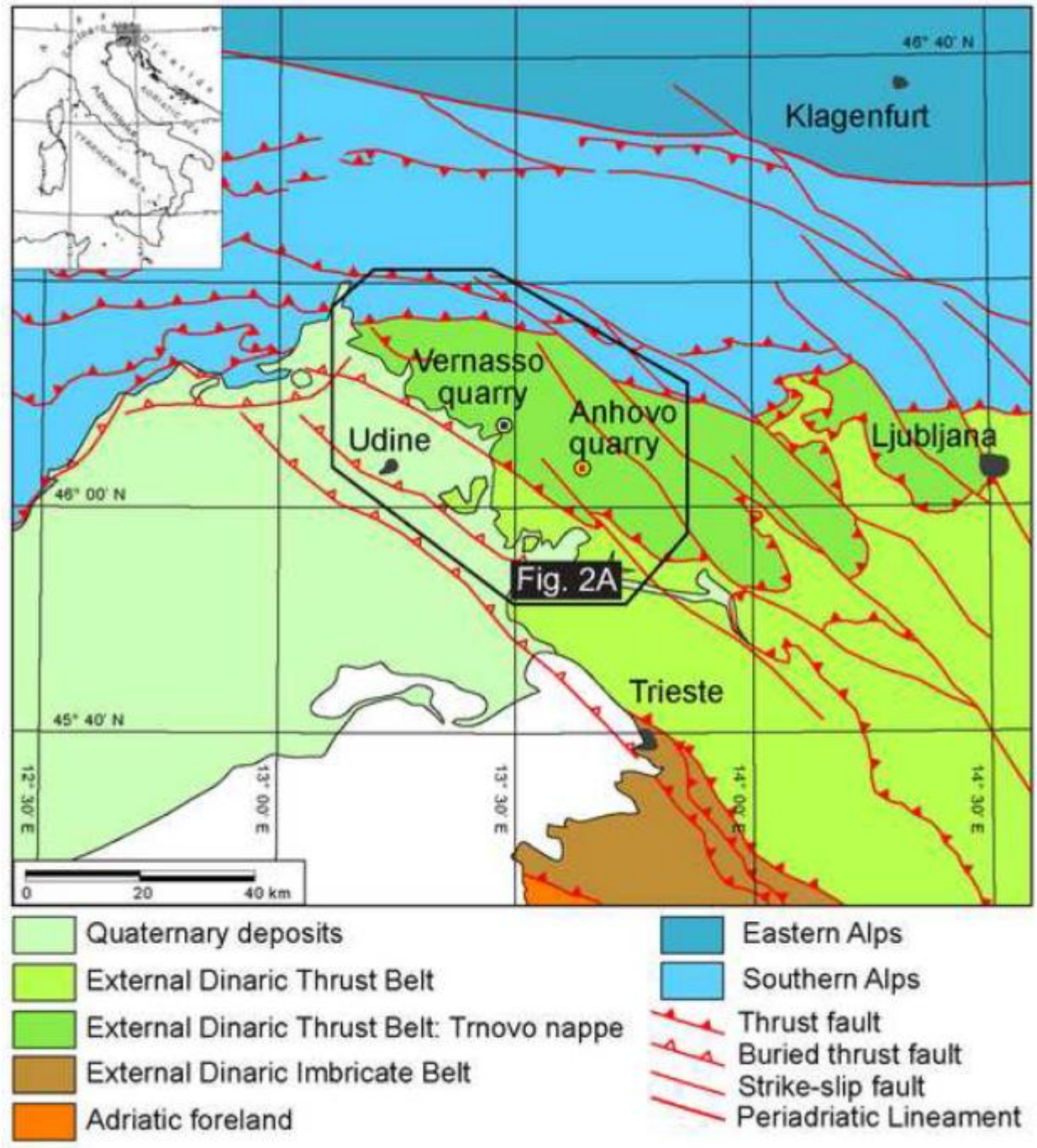

Figure2

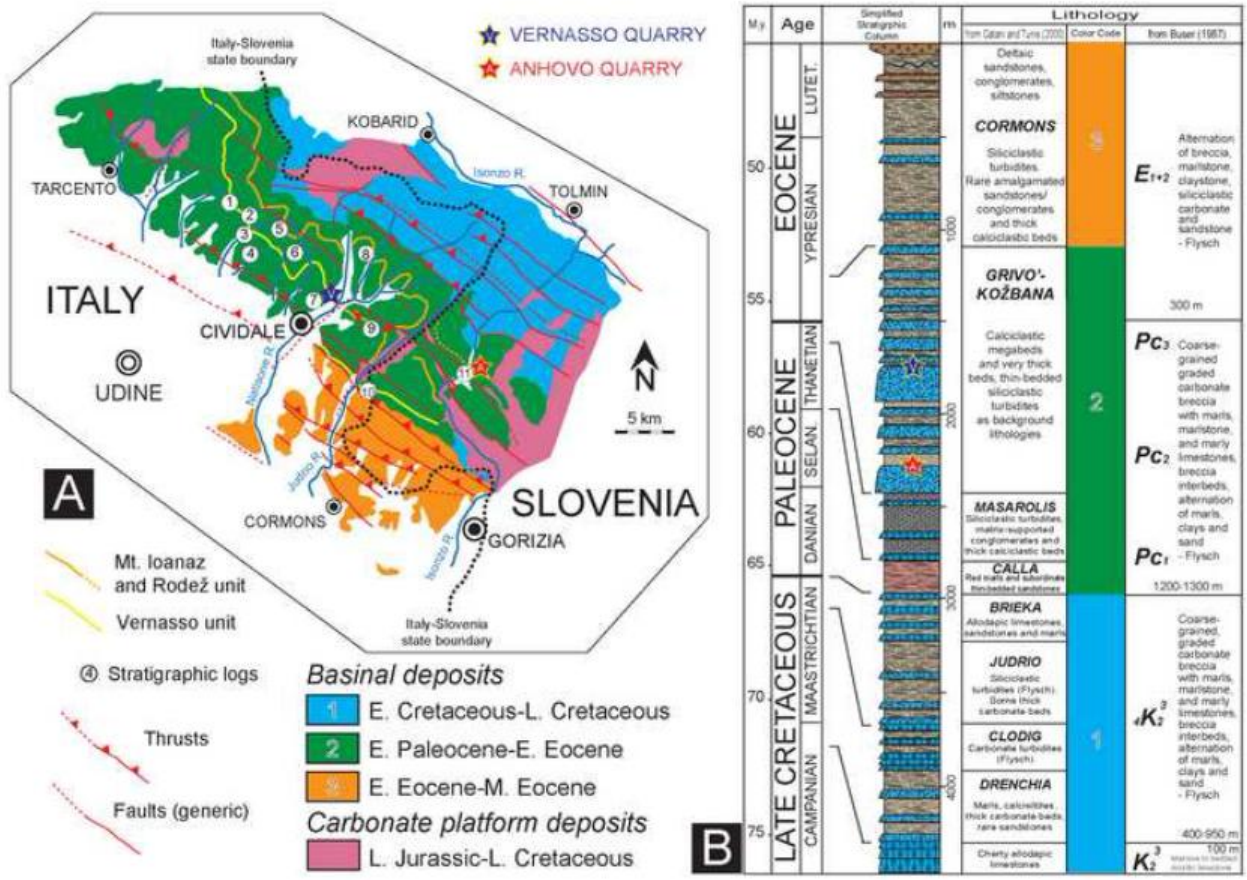

Figure3

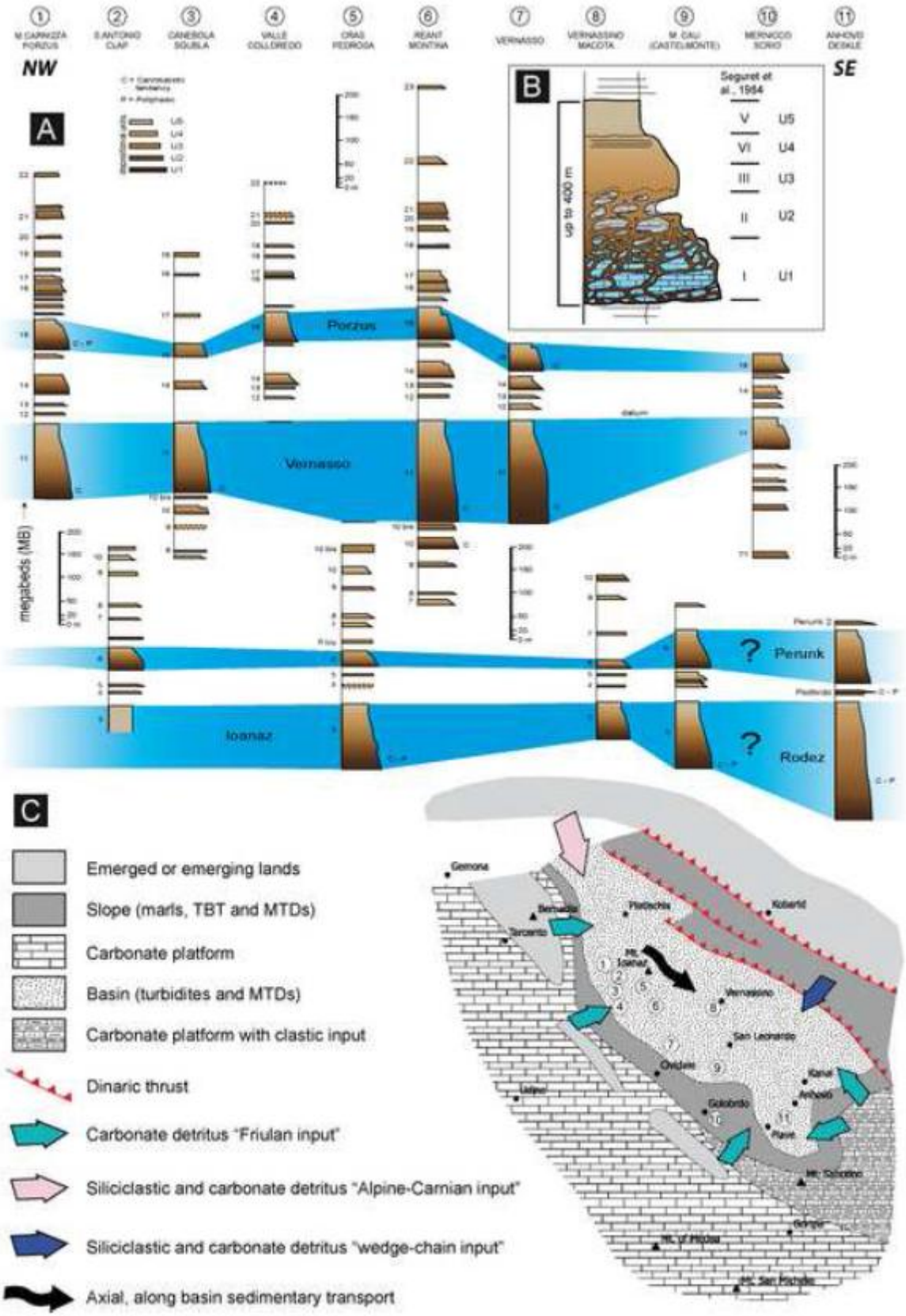

Figure4

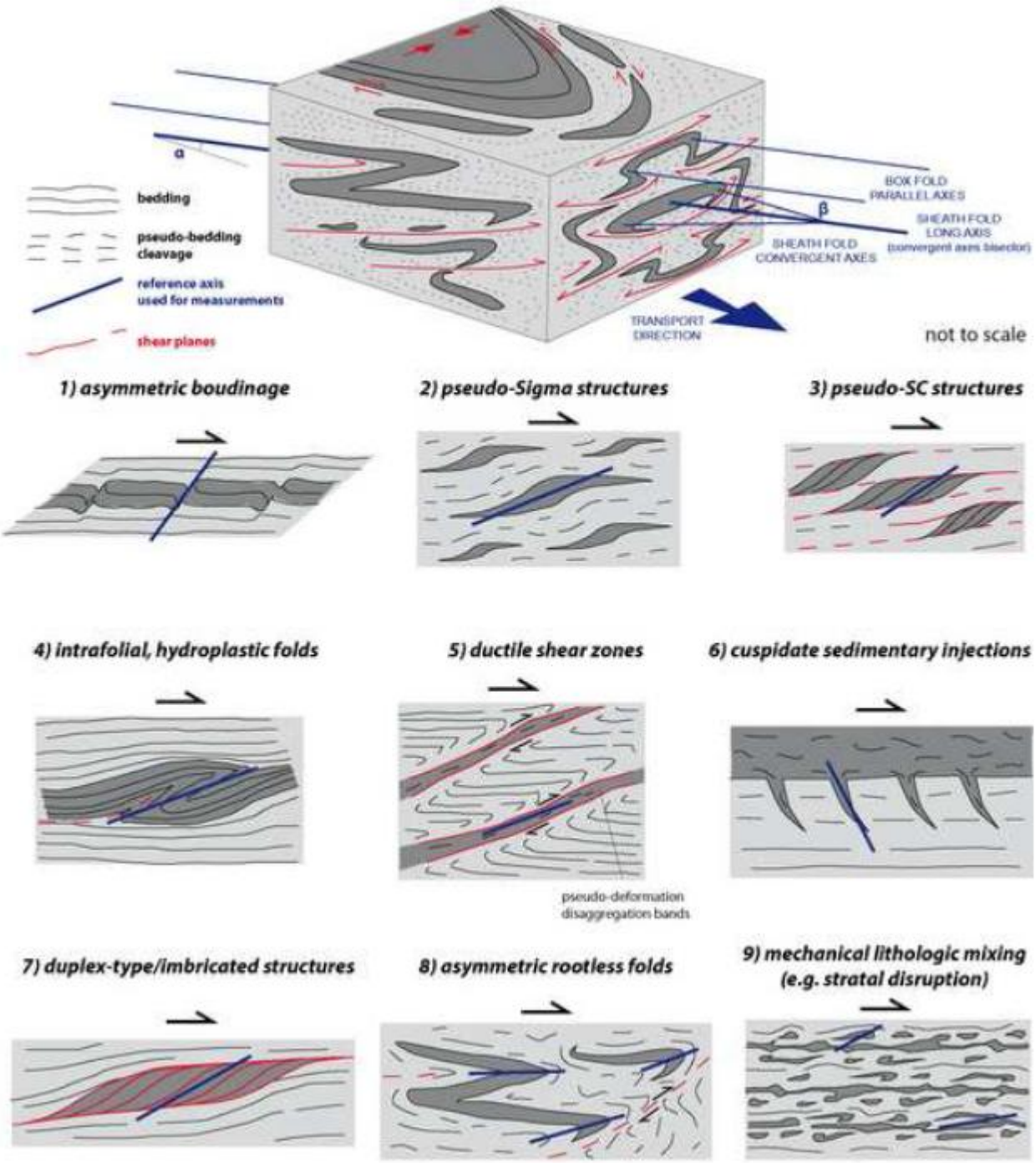

Figure5

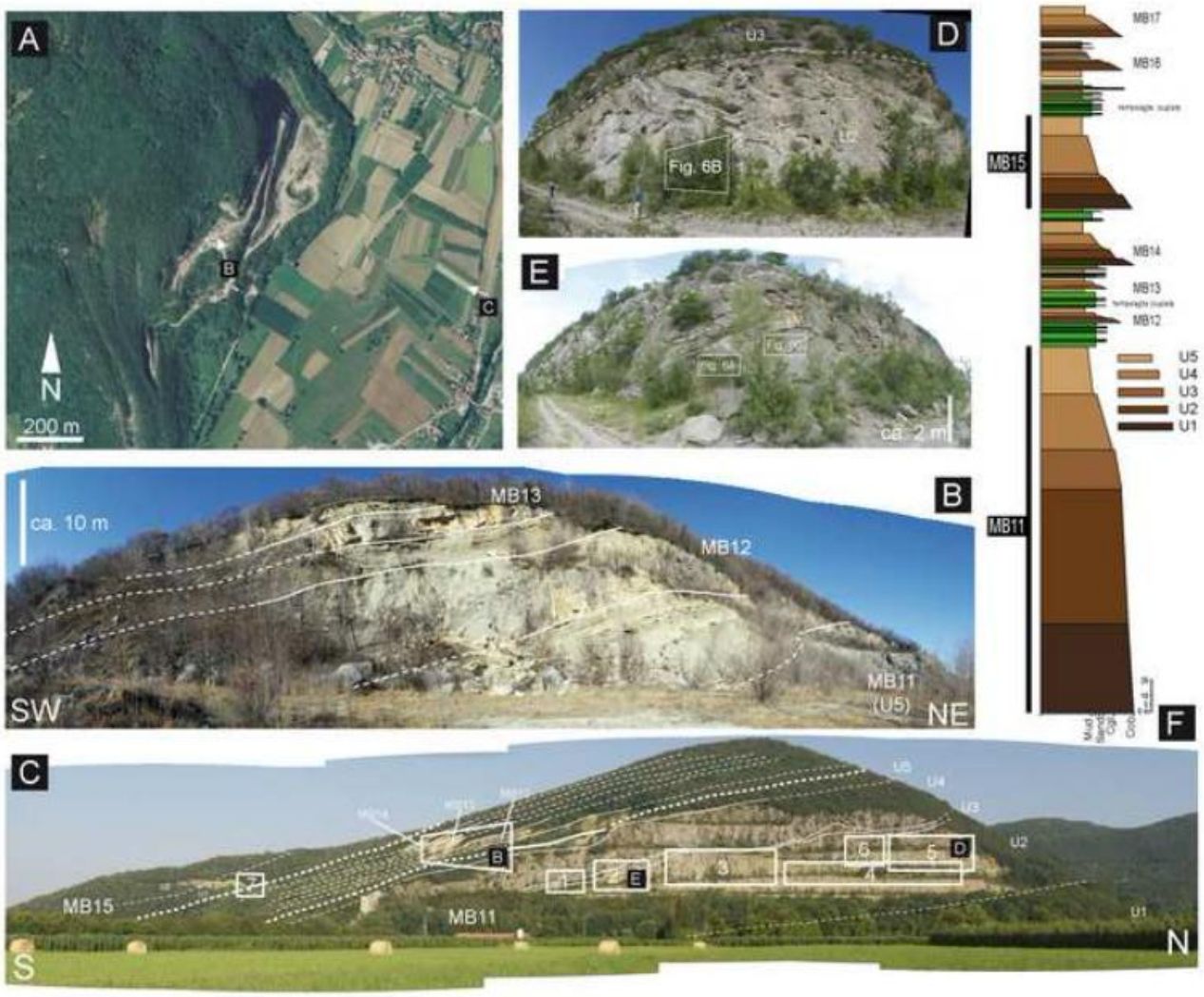

Figure6

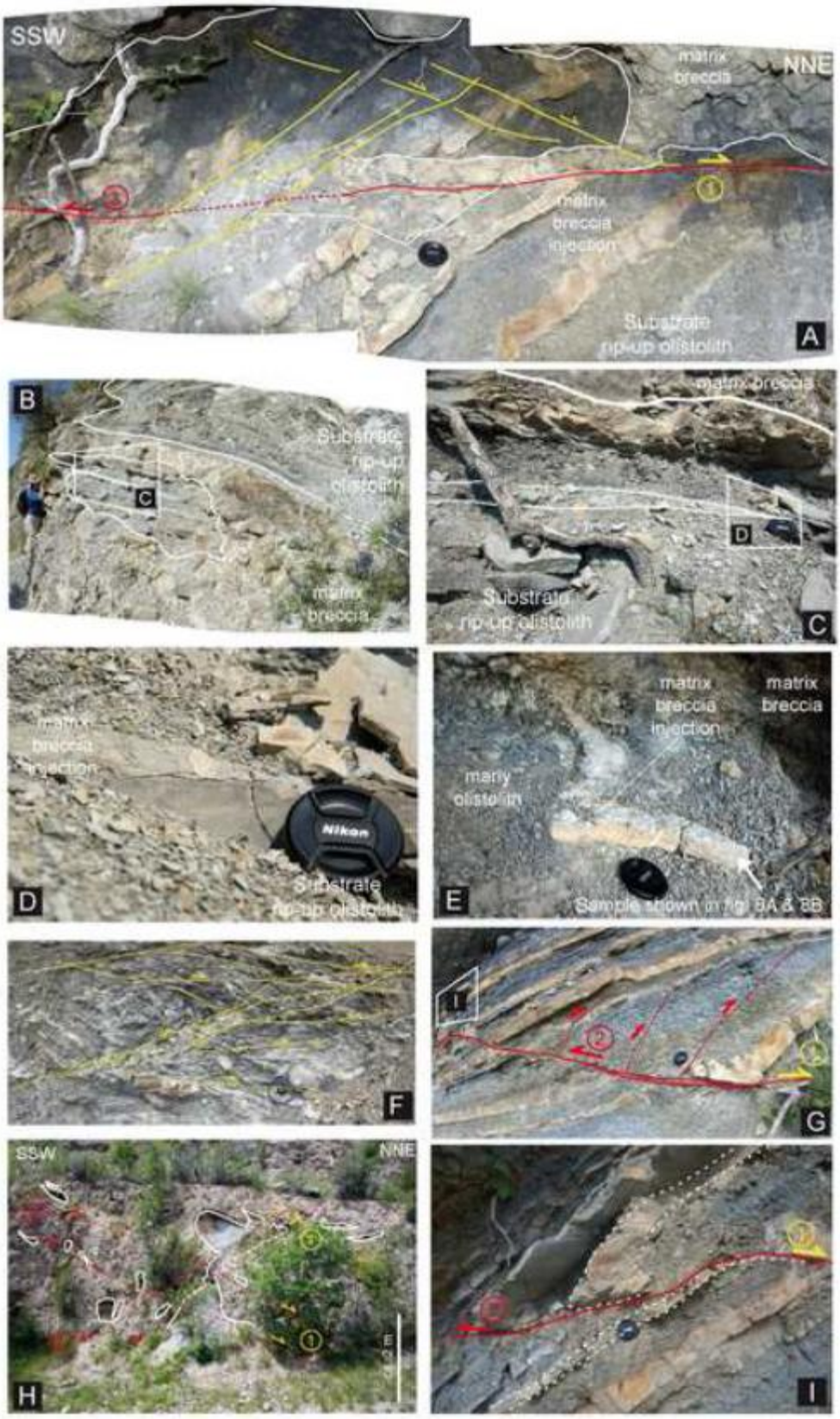

Figure7

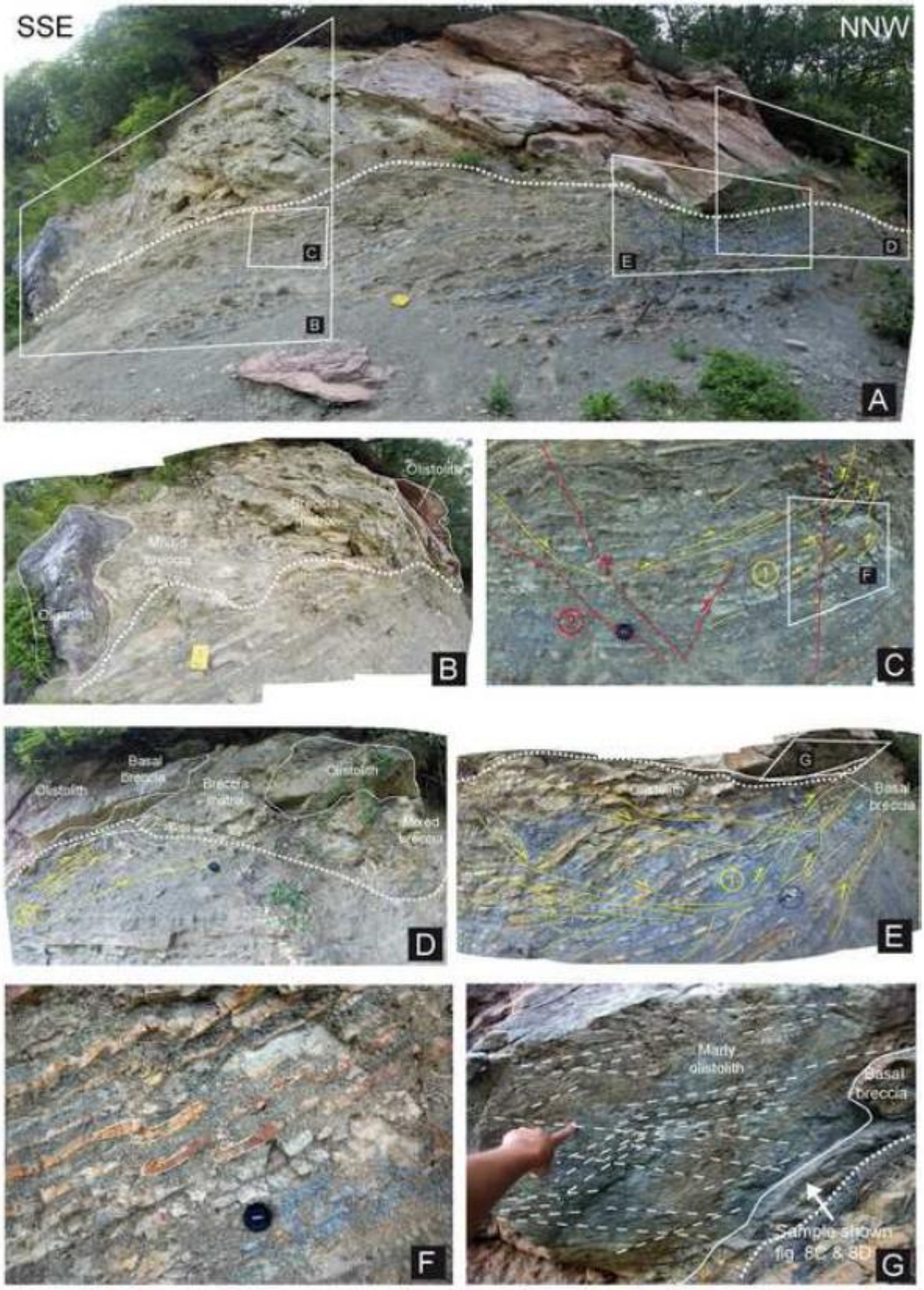

Figure8

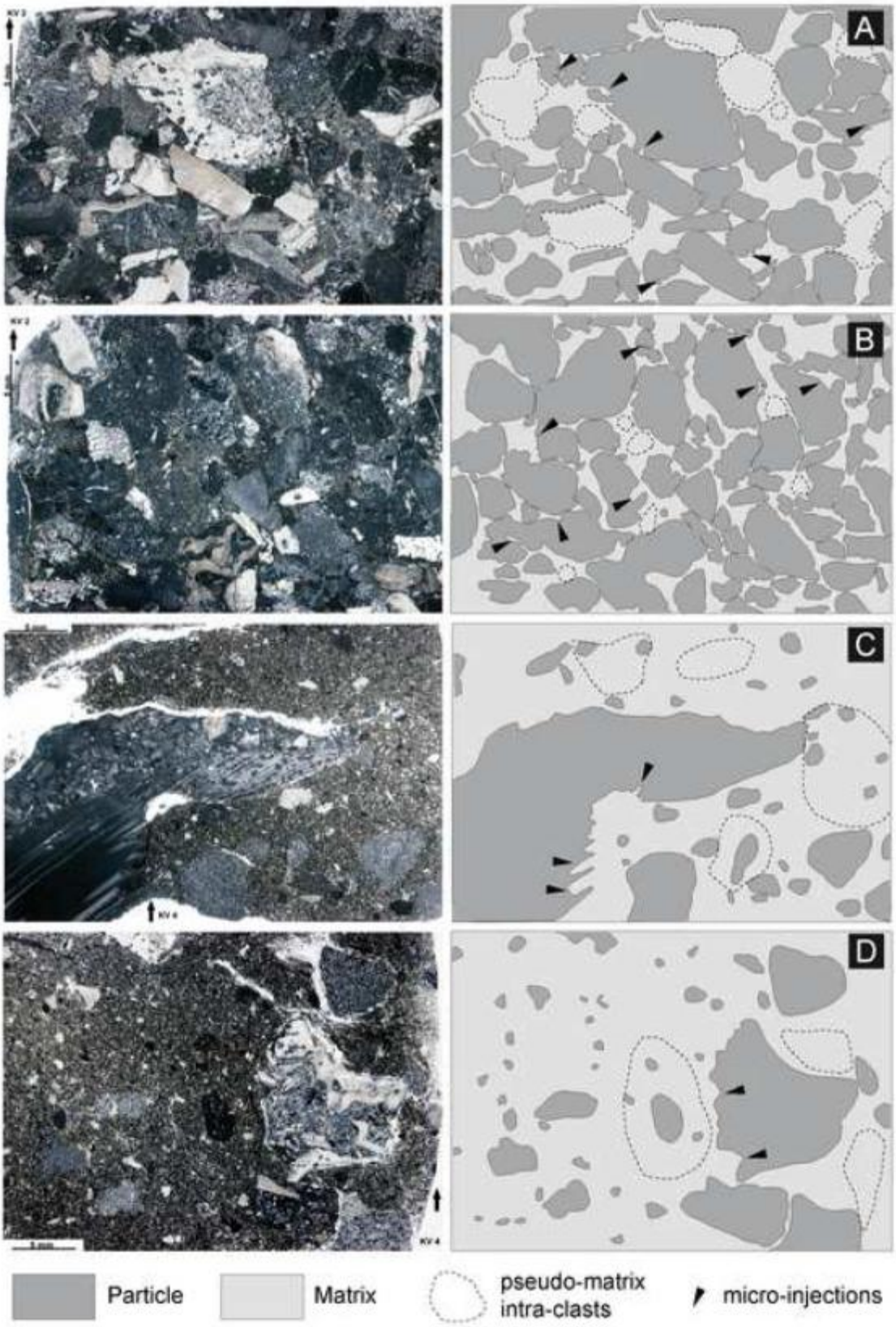

Figure9

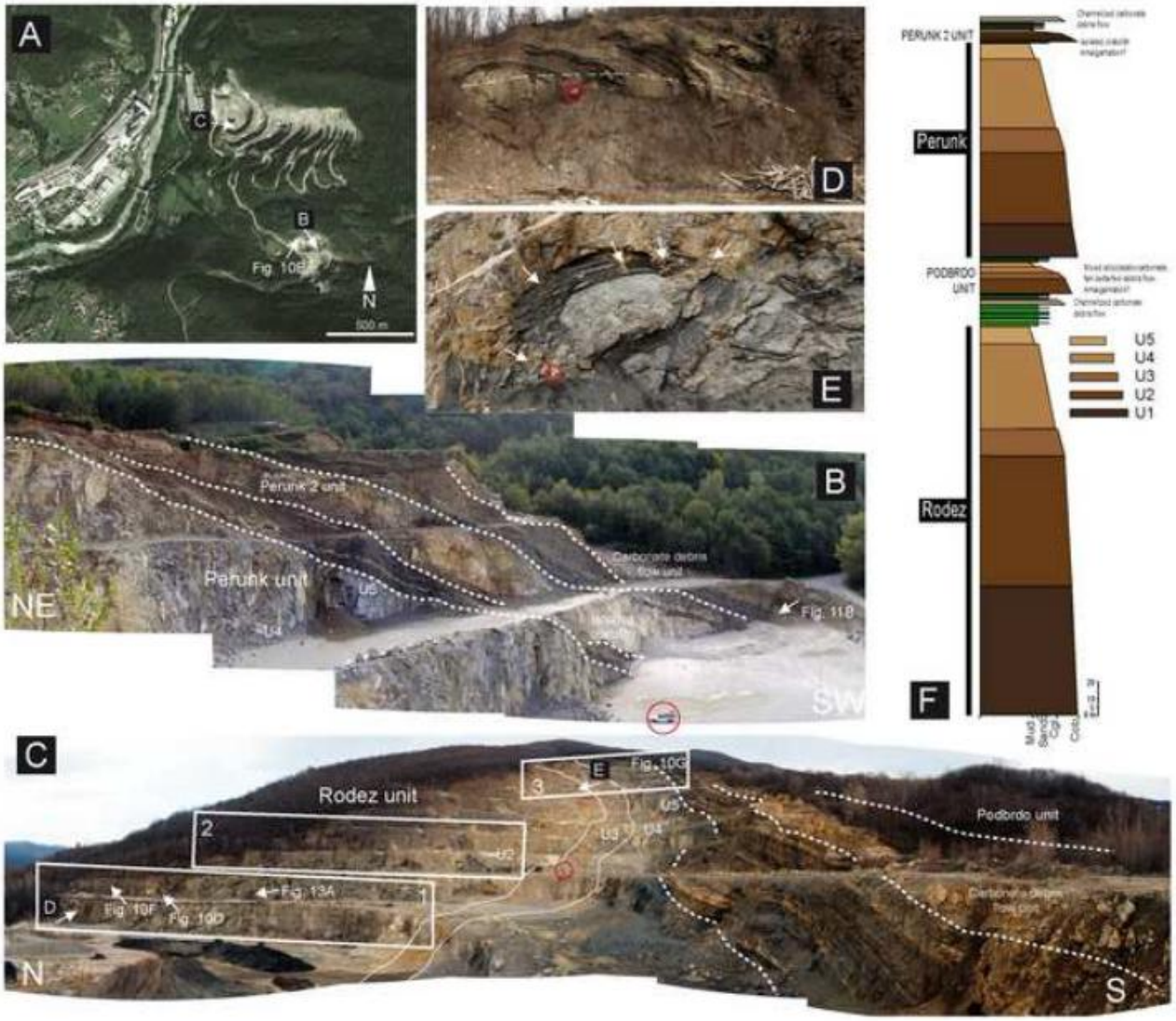

Figure10

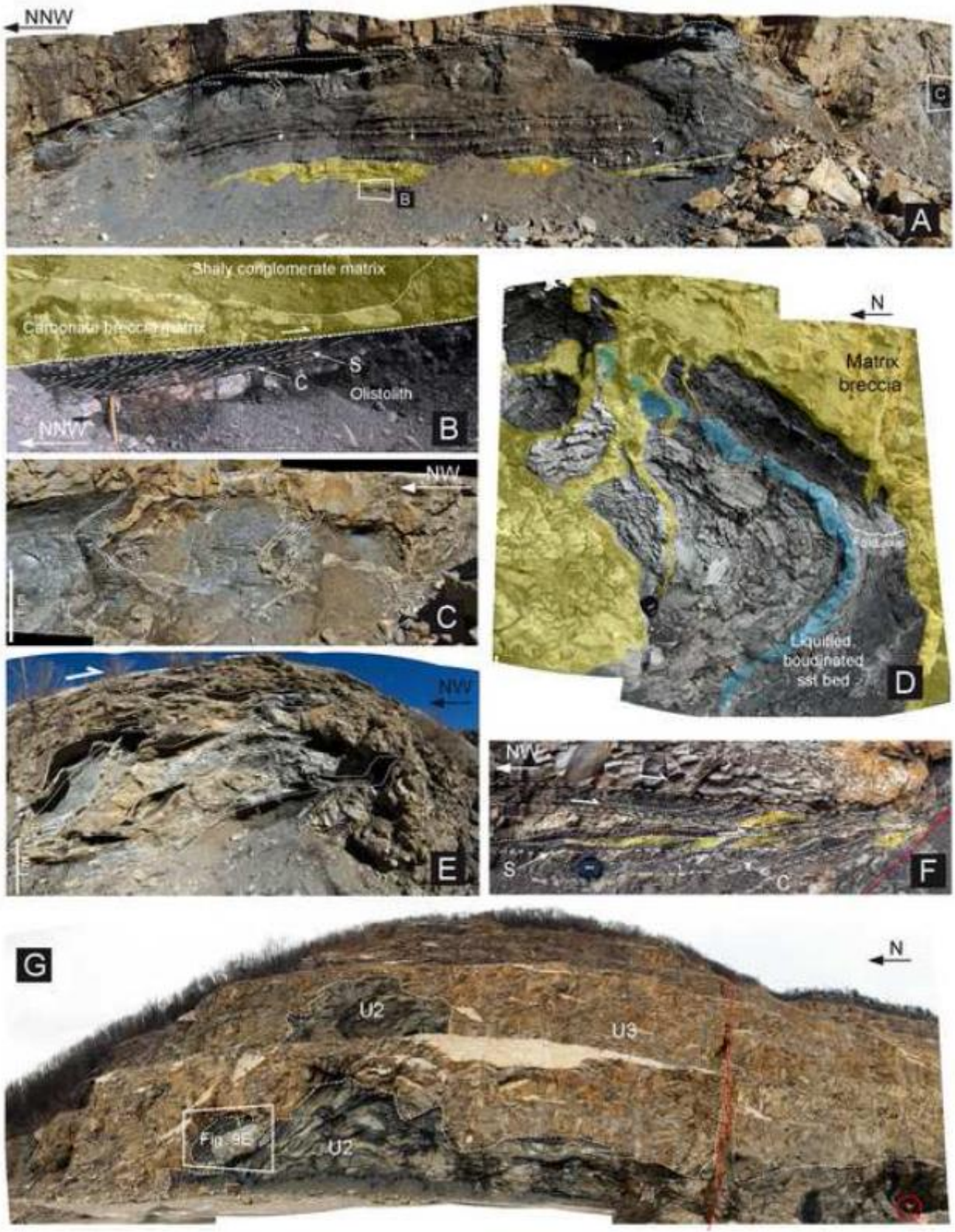

Figure11

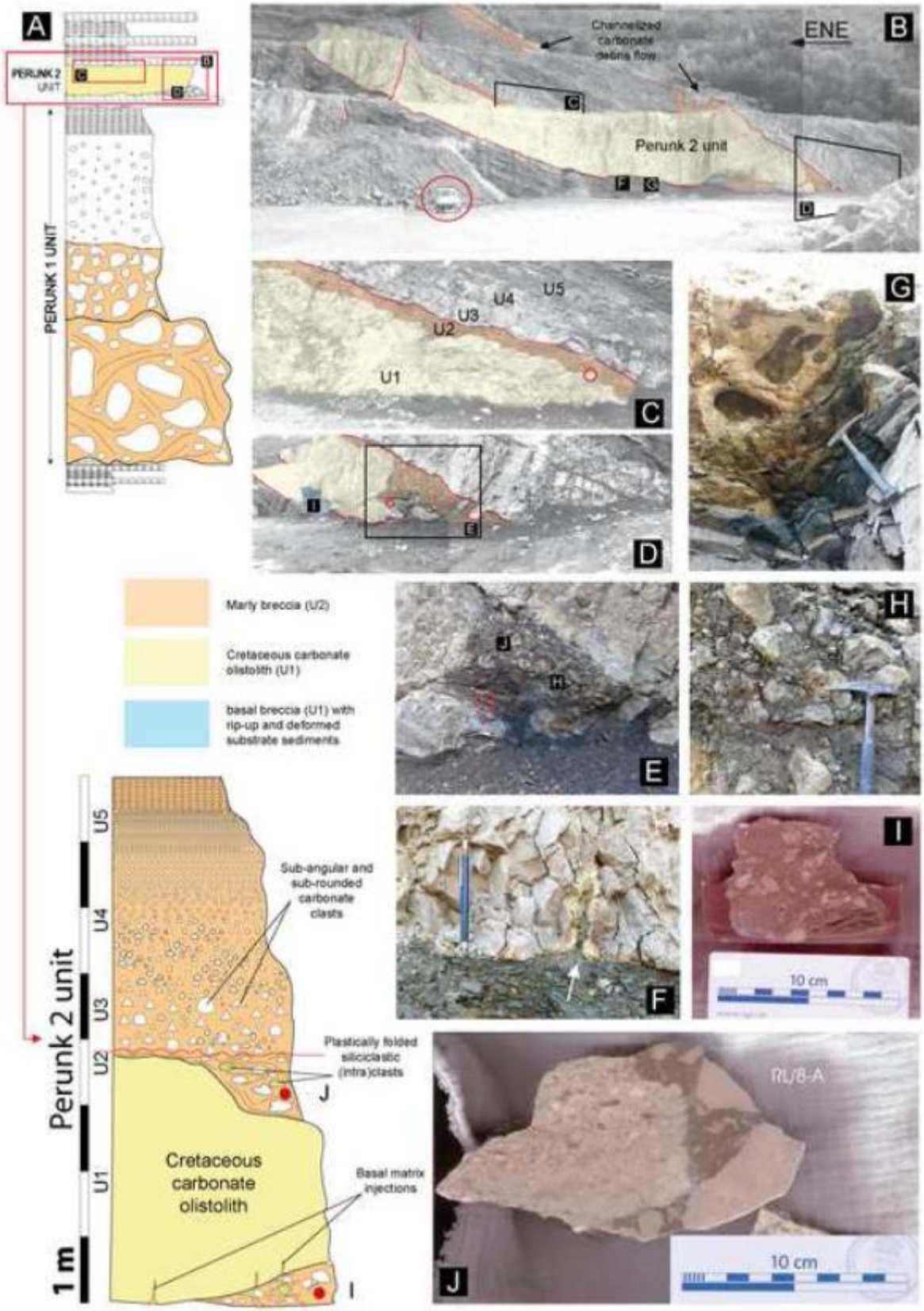

Figure12

Figure13

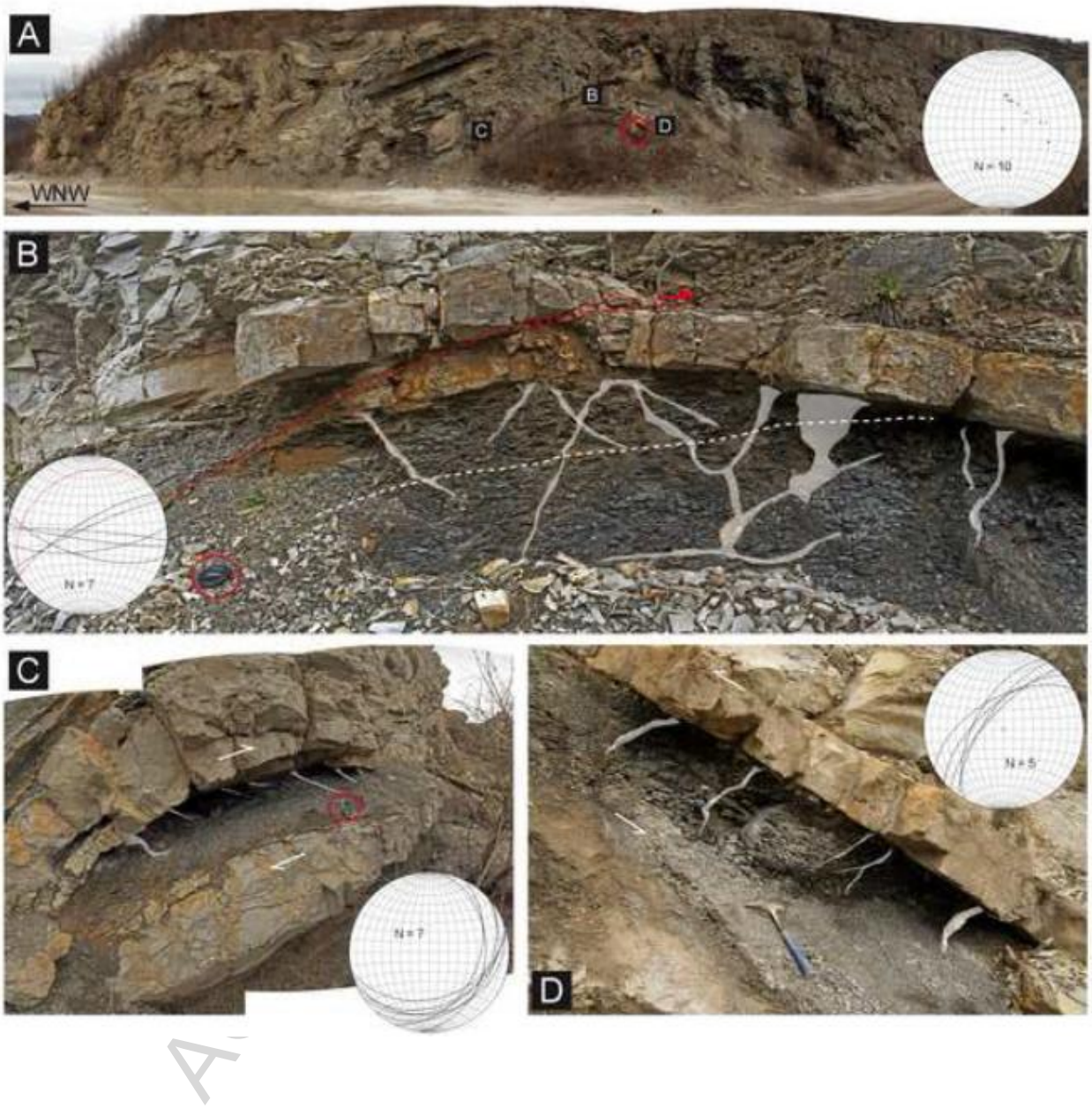

Figure14

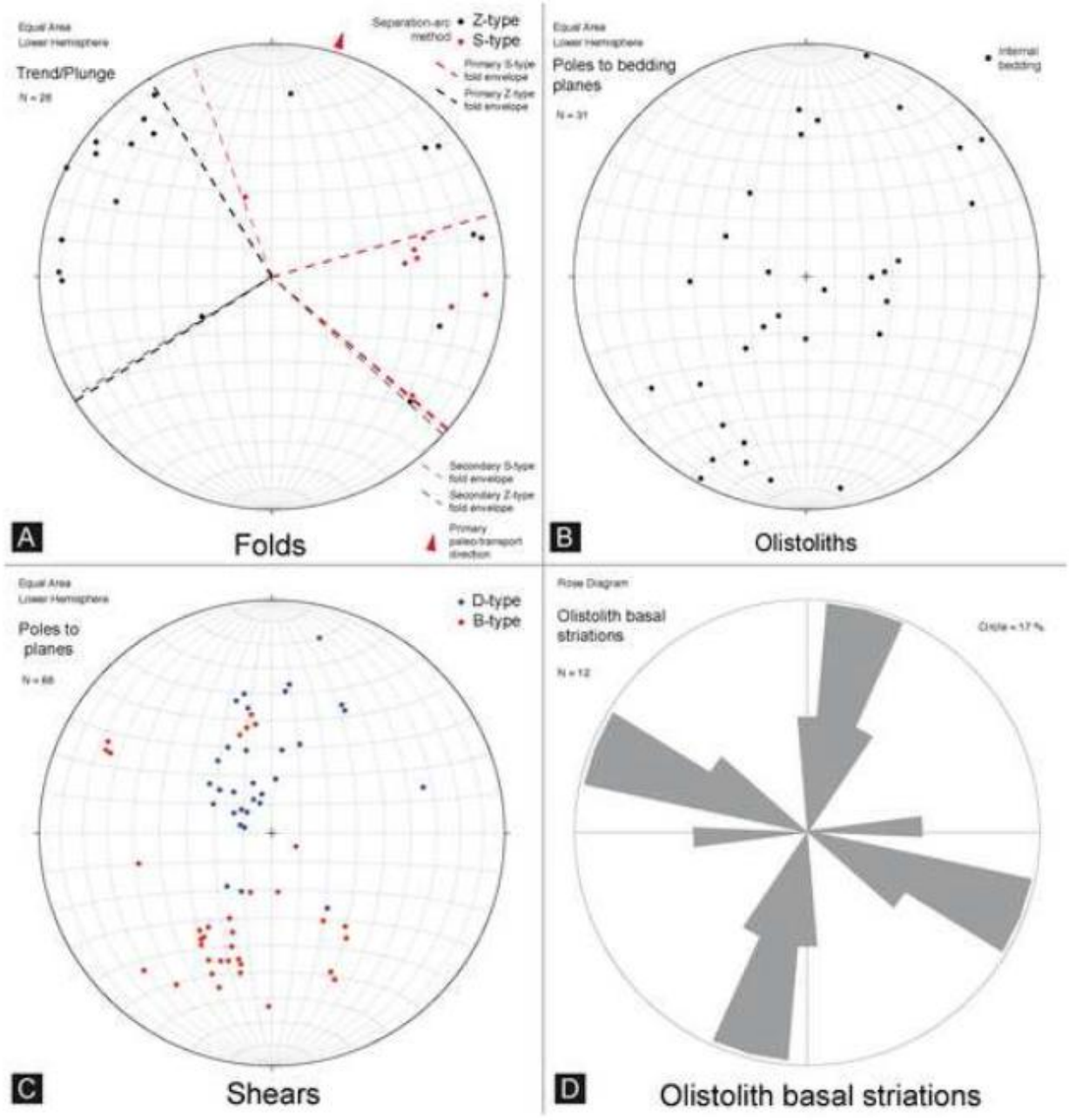

Figure15

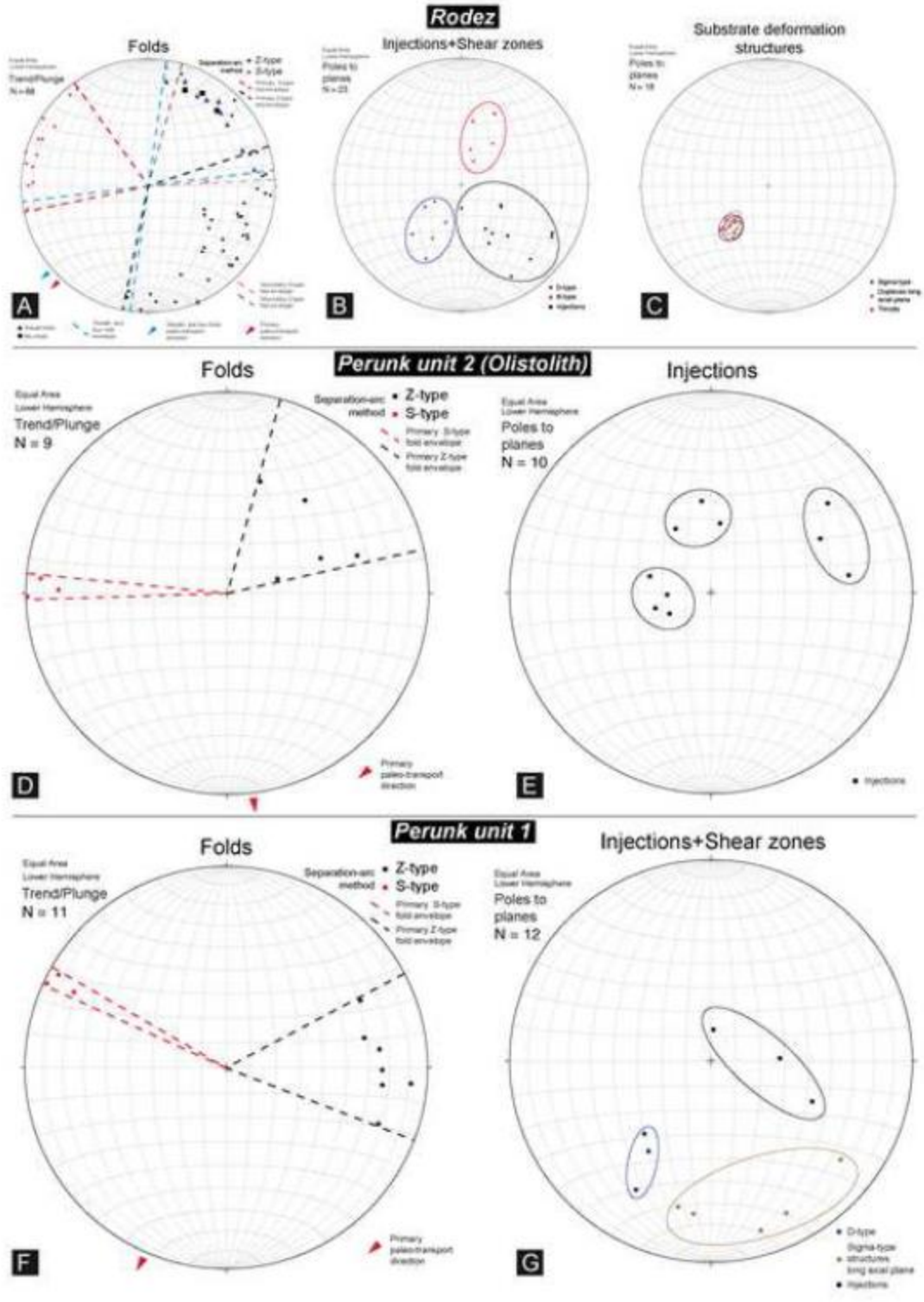

Figure16